Escola Superior de Tecnologia da Saúde do Porto

Instituto Politécnico do Porto

Anita Joana de Araújo Campos

Unraveling the role of microRNA-92 in Painful Diabetic Neuropathy

Mestrado: Bioquímica em Saúde, ramo de Biotecnologia

setembro de 2015

Mestrado de Bioquímica em Saúde

Dissertação de Mestrado

Unraveling the role of microRNA-92 in Painful Diabetic Neuropathy

Autora: Anita Joana de Araújo Campos

2º Ano do Mestrado de Bioquímica em Saúde

Nº 10130542

Dissertação submetida à Escola Superior de Tecnologia da Saúde do Porto para cumprimento dos requisitos necessários à obtenção do Grau de Mestre em Bioquímica em Saúde, no ramo de Biotecnologia realizada sob a orientação científica da Doutora Sandra Marisa Oliveira e coorientação do Doutor Rúben Fernandes.

setembro, 2015

Acknowledgments

First of all, to Doctor Carla Morgado for all work and time with me. To all skills and knowledge learned with her and for all care during this year.

My sincere thanks to my ERASMUS supervisor, Doctor Francesca Ruberti, leader group of the Institute of Cell Biology and Neurobiology from National Research Council in Italy, for their hospitality and for receiving me and provided me an opportunity to join their team and teach me new molecular techniques. To all the members of the research group: Doctor Christian Barbato for his kindness and motivation every day and to Maria Teresa Ciotti for her important role in the realization of all cell cultures in this thesis, and for the privilege of letting me see her meticulous work.

One special thanks to Doctor Daniela Posca, for being a friend during my ERASMUS internship and for all the knowledge shared.

I am sincerely grateful to all Department of Experimental Biology from Faculty of Medicine of Porto. In particular, to Professor Doctor Castro Lopes and Professor Doctor Isaura Tavares for allowing me to access their laboratory and research facilities. I would like to thanks also to my lab mates, Marta Louçano, José Oliveira, Rita Costa, Carla Abreu and Daniel Martins, who were the first to receive me with great care and kindness. To the department technicians, Elisa Nova and Fernando Martins.

To my co-supervisor Doctor and lecturer Rúben Fernandes, for accompanying me since my bachelor and support my educational lifetime decisions.

To my supervisor, Doctor Sandra Oliveira, an important person during this step of my life. For being patient and inspiring. For all help and motivation during my thesis writing, and to have the opportunity to learn from her great scientific knowledge.

To my friends Marta Gonçalves, Sofia Cabral, Joana Correia, Melissa Couto and Salomé Monteiro who accompanied me during this master and with me realized this step. For all conversations and unforgettable moments.

And last but most important, I have to be grateful to my lovely family, my mom, dad, brother, and boyfriend to the support they gave me during this step. This is for me and for them…

Resumo

A Diabetes é uma doença metabólica crónica caracterizada por hiperglicemia provocada por deficiências na secreção e/ou ação da insulina, associada a várias complicações, agudas ou crónicas, que afetam a qualidade de vida destes doentes. Uma das complicações crónicas mais comuns na diabetes é a Neuropatia Diabética Dolorosa (NDD), sendo a quinta principal causa de dor crónica em todo o mundo. A NDD é caracterizada por hiperalgesia mecânica e alodinia tátil e é acompanhada por alterações funcionais e neuroquímicas no sistema nervoso periférico e central. Atualmente, não existe tratamento eficaz para esta condição, sendo que se baseiam na prevenção e manutenção dos sintomas além de poderem apresentar efeitos secundários. Sabe-se que a disfunção nociceptiva espinhal durante a NDD é uma consequência da perda de ácido γ-aminobutírico (GABA), responsável pela inibição da dor, que está associada a uma reversão no fluxo neuronal de cloreto, induzida pela diminuição do co-transportador iónico potássio-cloro do tipo 2 (KCC2). Ratos diabéticos induzidos por estreptozotocina (STZ), exibem uma diminuição significativa na expressão do KCC2 na medula espinhal levando a um aumento da concentração intracelular de cloreto e a uma reversão do papel do GABA, de inibitório para excitatório. A inibição seletiva do miR-92, utilizando um vetor lentiviral, evita a diminuição da expressão de KCC2 no hipocampo. Considerando o papel do miR-92 sobre a regulação da expressão do KCC2 e as deficiências relatadas com este co-transportador na medula espinhal durante a diabetes, era importante avaliar se a inibição do miR-92 em ratos STZ seria uma possível terapia no alívio da dor, e avaliar o papel do KCC2 e do GABA como possíveis mediadores dos efeitos dessa inibição. Neste estudo, mostrou-se que a inibição do miR-92 em ratos diabéticos com neuropatia dolorosa aumentou a expressão do KCC2 e reduziu a nocicepção mecânica desses animais, o que aponta para um papel chave do miR-92 e do KCC2 na dor nociceptiva espinhal durante a NDD. Além disso, foi possível mostrar, através de um estudo farmacológico, que os resultados acima mencionados realmente dependem do KCC2 e do GABA, corroborando estudos anteriores. Foram ainda feitos estudos preliminares *in vitro*, para avaliar se a inflamação poderia estar a interferir a expressão de miR-2 e KCC2 neuronal. Embora os resultados não sejam conclusivos, sugerem um papel da inflamação na expressão do KCC2. Concluindo, este projeto identificou um potencial alvo terapêutico para a reversão das alterações na transmissão nociceptiva inibitória espinhal detetadas durante a NDD.

Palavras-Chave: microRNA-92, medula espinhal, neuropatia diabética dolorosa, nocicepção mecânica

Abstract

Diabetes Mellitus (diabetes) is a disease characterized by hyperglycemia resulting from defects in insulin secretion and/or its action, associated with several acute and chronic complications that affects the life quality of the patients. One of the most common complications of diabetes is Painful Diabetic Neuropathy (PDN), being the fifth main cause of chronic pain worldwide and causing a very debilitating condition. PDN is characterized by mechanical hyperalgesia and tactile allodynia and is accompanied by functional and neurochemical changes at peripheral and central nervous system. Currently, there are no efficient treatments for this disease since they are based on symptoms' prevention and management, and may present side effects. During PDN there is a loss of γ-aminobutyric acid (GABA)-mediated pain inhibition which was shown to be due to a reversal in chloride neuronal flux induced by the downregulation in K^+ Cl^- cotransporter 2 (KCC2). STZ-diabetic rats have been shown to exhibit a significant decrease in KCC2 expression at the spinal cord leading to an increase in chloride intracellular concentration and a reversal shift of GABA's properties. Recently, selective inhibition of miR-92, using a mir-92 sponge lentiviral vector approach was shown to prevent the decrease in KCC2 hippocampal expression. In this context, considering the role of miR-92 on the regulation of KCC2 expression and the impairments reported in this co-transporter in the spinal cord during diabetes, it is important to evaluate the possible pain-relieving therapeutic potential of silencing miR-92 in STZ-diabetic rats with PDN and to evaluate the role of KCC2 and GABA as possible mediators of the actions of silencing miR-92. In our study, it is shown that selective inhibition of miR-92 in STZ-diabetic rats with PDN, increases spinal cord KCC2 expression and reduces mechanical nociception, pointing for a key role of miR-92 and KCC2 in spinal pain abnormal nociceptive processing during PDN. Besides, it was possible to show, through a pharmacological study, that the results abovementioned depend on KCC2 and GABA, corroborating previous studies on their involvement in PDN. Preliminary *in vitro* studies were also undertaken to evaluate if inflammation may interfere with miR-92 and KCC2 neuronal expression. Although these preliminary results are not conclusive, they suggest a role for inflammation on KCC2 expression. In conclusion, this project has identified a potential therapeutic target for reversal of the excitatory changes in spinal nociceptive transmission occurring during PDN.

Keywords: miRNA-92, mechanical nociception, Painful diabetic neuropathy, spinal cord

Table of Contents

Abbreviations

BDNF: Brain derived neurotrophic factor

BIC: Bicuculline

DIOA: R-(+)-[(2-n-Butyl-6,7-dichloro-2-cyclopentyl-2,3-dihydro-1-oxo-1H-inden-5-yl)oxy] acetic acid

DMSO: Dimethyl sulfoxide

EGFP: Enhanced green fluorescent protein

GABA: γ-aminobutyric acid

$GABA_AR$: GABA A receptors

HEK: Human Embryonic Kidney

HRP: Horseradish peroxidase

IL-1β: Interleukin 1β

KCC2: Potassium-chloride cotransporter type 2

miR-92: MicroRNA-92

MRE: microRNA responsive elements

NKCC1: Sodium-Potassium-chloride cotransporter type 1

OFT: Open field test

PBS: Phosphate buffer saline

PDN: Painful Diabetic Neuropathy

PPT: Paw pressure test

PWT: Paw withdrawal threshold

RISC: RNA-induced silencing complex

RNO: *Rattus norvegicus*

RT-PCR: Real-Time polymerase chain reaction

RVM: Rostral ventromedial medulla

SDS: Sodium dodecyl sulfate

SDS-PAGE: Sodium dodecyl sulfate – Polyacrylamide gel eletrophoresis

STZ: Streptozotocin

TBP: Tata box binding protein

TGS: Tris-glycine SDS

TNF-α: Tumor necrosis factor α

List of Figures

I. Introduction

1. Diabetes Mellitus

Diabetes Mellitus (diabetes) is a disease characterized by hyperglycemia resulting from defects in insulin secretion and/or its action. There are three main types of diabetes: type 1 diabetes, type 2 diabetes and gestational diabetes. In type 1 diabetes, there is an absolute deficiency of insulin secretion, caused by an autoimmune destruction of pancreatic β-cells. Primary symptoms of hyperglycemia of type 1 diabetes include polyuria, polydipsia, weight loss, polyphagia and blurred vision. Commonly, this immune-mediated diabetes occurs in childhood and adolescence. Some forms of type 1 diabetes have unknown etiologies, namely idiopathic diabetes. In type 2 diabetes, the most prevalent type of diabetes (~90-95% of those with diabetes), the cause is, very often, a combination between resistance to insulin action and inadequate compensatory insulin secretory response. During the development of this type of diabetes, damage in tissues can occur without noticeable clinical symptoms for a long period before its detection. Obesity or an increase body fat distributed predominantly in the abdominal region are among the various possible causes of this type of diabetes, as well as stress and other illness, such as infection. Gestational *diabetes mellitus* (GDM) is defined as any degree of glucose intolerance with onset or first recognition during pregnancy. However, this type of diabetes was controversial for many years, since its diagnosis could not be done accurately, being some cases of GDM preexisting undiagnosed type 2 diabetes (American Diabetes, 2014; Skyler, 2004).

2. Epidemiology of Diabetes

Diabetes is the most common metabolic chronic disorder in nearly all countries and continues to increase. This year, the International Diabetes Federation published the numbers of diabetes prevalence for 2013 in global scale. In Europe, prevalence of diabetes in the population aged between 20 and 79 years old was 7,9%, in Eastern Mediterranean and Middle-East was 9,7% and North America presented the largest number of 11, 4% (Guariguata et al., 2014). In Portugal, the estimated prevalence of diabetes in 2013 was 13%, more than 1 million of Portuguese population, and more 1,3% than first study made of prevalence in 2009. More worryingly, the prevalence of diabetes is rising due to increased obesity, changes in diet, lifestyle, and population ageing (Diabetologia, 2014; Gardete-Correia et al., 2010; Guariguata et al., 2014).

3. Painful Diabetic Neuropathy: a Complication of Diabetes

Diabetes involve several medical complications, some of them affecting with severity life quality of these patients. Complications can be divided in acute and chronic complications. Within acute complications, individuals with diabetes can lead with diabetic ketoacidosis, hyperglycemic hyperosmolar state, hypoglycemia and infections in different locations (respiratory system, genitourinary, gastrointestinal and liver, head, skin) (Lamster, 2014). Chronic or long-term complications of diabetes include microvascular and macrovascular complications. Severe retinopathy, nephropathy, peripheral and autonomic neuropathy, and diabetic foot are the most common microvascular complications. Into macrovascular complications there are the coronary heart disease, cerebrovascular and peripheral arterial disease (American Diabetes, 2014; Lamster, 2014).

Diabetic neuropathy (DN) is one of the most common chronic debilitating complications of diabetes, affecting more than 50% of diabetic individuals (Lamster, 2014; Tesfaye et al., 2010). On

the other hand diabetes is the leading cause of neuropathy, defined as damage to the nerves of the peripheral nervous system (Callaghan, Cheng, Stables, Smith, & Feldman, 2012). DN can be classified into four main classes based on symptoms and their location: (1) distal symmetric polyneuropathy (DSPN); (2) autonomic neuropathy; (3) proximal motor neuropathy; and (4) focal mononeuropathy and multifocal (Lamster, 2014).

- **Classifications of diabetic neuropathies:**

(1) Diabetic distal symmetric polyneuropathy, also called diabetic peripheral neuropathy, is the most common DN and can be found in both type 1 and type 2 diabetes (Callaghan et al., 2012; Kazamel & Dyck, 2015). This form of DN affects up to 50% of the individuals with diabetes and is characterized by pain, paresthesia, hyperesthesia, deep aching, burning, and sensory loss (Kazamel & Dyck, 2015; Tesfaye & Selvarajah, 2012). DSPN affects the nerves of extremities such as feet and hands, but symptoms can progress proximally (Ahmad & Mittal; Kazamel & Dyck, 2015; Lamster, 2014).

(2) Autonomic neuropathy affects autonomic nervous system that controls automatic actions from the organs. This type of neuropathy can cause dysfunction of cardiovascular, gastrointestinal, genitourinary, sudomotor and metabolic systems affecting body's homeostasis (Lamster, 2014).

(3) Proximal motor neuropathy or diabetic amyotrophy is the less common, and mostly affects older individuals with type 2 diabetes (Lamster, 2014). This kind of neuropathy can cause muscle weakness and affects specially the upper muscles of legs and hips (American Diabetes, 2009; Diseases, Digestive, & Kidney, 2015).

(4) Focal neuropathy or mononeuropathy affects only one nerve unlike the above-mentioned neuropathies and can occur in medial, ulnar, radial and common

peroneal nerves (Boulton et al., 2005; Dyck et al., 2011). Multiple mononeuropathies are namely multifocal and the entrapment or compression of the nerves are commonly the cause (Kazamel & Dyck, 2015).

Of 50%-60% of diabetic patients who develop neuropathy, about 25%-30% develop painful symptoms, mainly associated with DSPN (Tesfaye, Boulton, & Dickenson, 2013). This very debilitating condition is called painful diabetic neuropathy (PDN) and makes this metabolic disease the fifth main cause of chronic pain (Tesfaye et al., 2010; Tesfaye & Selvarajah, 2012). PDN affects sensory, autonomic and motor neurons of the peripheral nervous system, thus covering all types of nerve fibers. This complication severely affects patients' quality of life, especially in those that pain appears as a major complaint in patients with PDN, pain is the most prominent and most frequent reason for searching health care professionals. PDN is defined by the International Association for the Study of Pain (IASP) as the 'pain arising as a direct consequence of abnormalities in the somatosensory system in people with diabetes'. Hyperalgesia (exacerbated pain to noxious stimulation) and allodynia (pain induced by innocuous stimuli) are frequently present. The symptoms often described by patients with PDN include: burning pain, 'electrical shock' type shooting pain down the legs, lancinating pain, uncomfortable tingling, pain caused by touching clothes (allodynia), discomfort on walking and sensitivity to temperature changes (Duby, Campbell, Setter, White, & Rasmussen, 2004; Shakeel, 2014; Tesfaye, Vileikyte, Rayman, Sindrup, Perkins, Baconja, Vinik, Boulton, et al., 2011). These symptoms are more severe at night and often interferes with normal sleep (Tesfaye et al., 2013).

3.1. Modulation of Pain

As illustrated in Figure 1, the sensory experience begins in the peripheral terminals of primary afferent fibers which respond to a countless of stimuli and translate this information into the dorsal horn of the spinal cord, where terminals of these fibers end. In the peripheral nervous system, three main types of sensory fibers exist: Aβ-fibers, Aδ-fibers, and C-fibers.

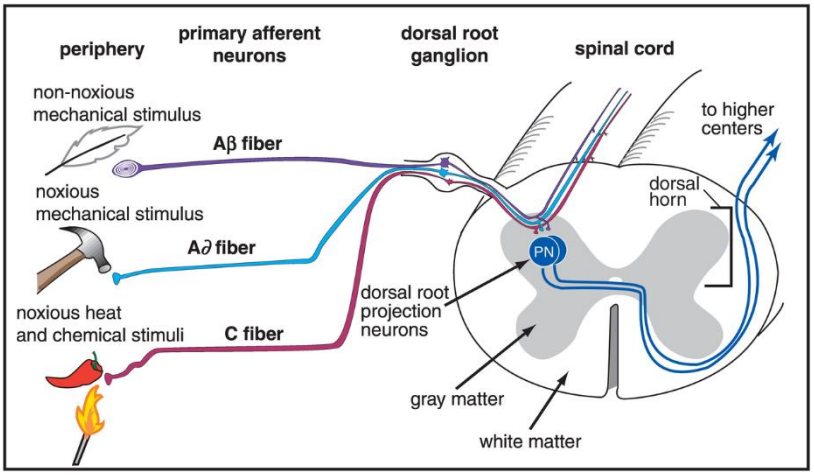

Figure 1 – Detection, at the primary afferents neurons, of different stimuli by nociceptive fibers. (Stahl, 2013)

Each of these fibers corresponds to the axons of first-order sensory neurons and has different properties that allow them to respond and transmit different types of sensory information. Aβ-fibers are thicker and highly myelinated, allowing them to quickly conduct action potentials from their peripheral to central terminals. These fibers normally respond to light touch and are responsible to transmit tactile information. Aδ-fibers are thinner, lightly myelinated, and consequently slower conducting. They respond to both thermal and mechanical stimuli. C-fibers are the smallest and are unmyelinated, thus being the slowest conducting. They detect selectively nociceptive or 'painful' stimuli (D'Mello & Dickenson, 2008). From here, the sensory fibers can take two main nociceptive ascending pathways, the lemniscal or the spinothalamic (Stahl, 2013). In the lemniscal pathway, responsible for touch and proprioception, the Aβ- and Aδ-sensory fibers can connect their axons of first-order to the axons of second-order in the medulla (Stahl, 2013; Tavares, Lima, & Almeida,

2014). Then, the axon of second-order neuron crosses the midline and follows the pathway to the thalamus where it connects with the axon of third-order neuron. In the spinothalamic pathway, the transmitted information refers to pain, temperature and rough touch. In this pathway, the axons of the first-order neuron coming from Aδ- and C-fibers transmits their impulses to the axon of the second-order neuron in the dorsal horn of the spinal cord. The side of the spinal cord to which the first-order neuron enters corresponds to the side from where the impulse was transmitted. This neuron then crosses the spinal cord midline and follows the pathway connecting to the axon of third-order neuron in the thalamus. In both pathways, the third-order neuron sends its axon to the thalamus, which in turns projects to cortical areas such as the somatosensory, anterior cingulate and insular cortices that are required for the conscious perception of pain (Tavares et al., 2014). Descending modulation starts from this point, when the cortical areas modulate the experience of pain and send their stimuli responses. These outputs are then sent to the periaqueductal grey (PAG) that communicates with the rostral ventromedial medulla (RVM) which, in turn, sends descending inhibitory or facilitatory projections to the spinal cord (Ossipov, Dussor, & Porreca, 2010). Furthermore, there are also excitatory, glutamatergic, and inhibitory, GABAergic and glycinergic interneurons inside the spinal cord and these can increase or decrease the response of nociceptive specific cells influencing the output of the dorsal horn (D'Mello & Dickenson, 2008; Tesfaye et al., 2013).

In neuropathic pain, repeated noxious inputs on nociceptive specific cells induced changes that will emphasize peripheral and central sensitization, which may result in disruption of antinociceptive system and exacerbation of pronociceptive system. These changes can lead to increased responses to a stimulus that is normally painful—hyperalgesia, or to a pain response to a stimulus that does not normally provoke pain—allodynia (Almeida, Leite-Almeida, & Tavares, 2006; McMahon, Koltzenburg, Tracey, & Turk, 2013).

3.1.1. Pain Processing in the Spinal Cord

Over the past two decades, research in understanding the pathophysiological neural changes resulting in neuropathic pain increased dramatically. Such changes include alterations in the (1) excitability or activation threshold of primary sensory neurons, (2) increases in descending facilitation or decreases in descending inhibition from the brain, and (3) increases in excitatory signaling or decreases in inhibitory signaling in the dorsal horn of the spinal cord (Taylor, 2009).

Descending inhibition of spinal nociceptive processing from the RVM was early studied and was the main focus of investigation for a long time. However, Frank Porreca and Alan Randich (Porreca, Ossipov, & Gebhart, 2002), from the University of Iowa, established the presence of descending facilitation in spinal nociception, and later, with Mark Urban (Pogatzki, Urban, Brennan, & Gebhart, 2002), they established a role for the RVM in the maintenance of hyperalgesic states following peripheral tissue injury. Using chemical stimulation, it was demonstrated that low concentrations of glutamate facilitate nociceptive processing while higher concentrations inhibit it. GABA and glycine are the main inhibitory neurotransmitters used by inhibitory neurons in the spinal cord dorsal horn. In most neurons, both neurotransmitters inhibit neuronal activation by hyperpolarizing the cell membrane and by activation of a shunting conductance, which impairs propagation of excitatory postsynaptic potentials along the dendrites of neurons (Zeilhofer, 2008).

3.1.1.1 Role of Potassium-Chloride Co-transporters

It is known that fast synaptic transmission depends on ion fluxes, and its efficacy is maintained through balance of transmembrane ionic gradients (Chamma, Chevy, Poncer, & Lévi, 2012). Chloride homeostasis depends on two cation-chloride co-transporters: sodium-

potassium-chloride co-transporter 1 (NKCC1) and the potassium-chloride co-transporter 2 (KCC2). Their effectiveness is reflected in the control of inhibitory transmission and its proper functioning. The most important inhibitory neurotransmitters in the adult mammalian spinal cord, GABA and glycine, depend on the gradient between intracellular and extracellular chloride concentrations to perform their action. In 2009, A.Stil et al. studied NKCC1 and KCC2 during the development of rat embryos and discovered that maturation of chloride homeostasis is not completed at birth and, at the same time (Stil et al., 2009). Moreover, from embryo to adult, NKCC1 and KCC2 levels suffer variations. In early developmental, NKCC2 levels are high in contrast to KCC2 levels, making NKCC1 the main chloride-potassium co-transporter in the brain. In the adult stage, NKCC1 decreases and KCC2 increases, leading with a reduction in the influx of chloride and a shift on its gradient (Price, Cervero, & de Koninck, 2005; Rivera et al., 1999).

Hereafter, we will focus our attention on KCC2, since it has been shown to have a major role in the nociceptive neurons of the superficial spinal dorsal horn in chronic pain (Coull et al., 2003; Mantyh & Hunt, 2004; W. Zhang, Liu, & Xu, 2008). Besides, studies analyzing the spinal cord of diabetic rats showed that KCC2 (but not NKCC1) is decreased in this condition (Jolivalt, Lee, Ramos, & Calcutt, 2008; Lee-Kubli & Calcutt, 2014), making KCC2 more relevant for our studies. KCC2 is a secondary active transporter that uses the energy of the electrochemical K^+ gradient to transport Cl^- and this way controls the electrochemical gradient of chloride ions in neurons. An increase in KCC2 concentration correlates with a progressive hyperpolarization of GABA reflecting a reduction of Cl^- concentration in mature neurons. An experiment using knockout animals for KCC2 gene, verified that in the absence of KCC2 expression spine morphogenesis is compromised in immature neurons. This defect on spine maturation is associated with a reduced number of functional excitatory synapses as detected by a decreased density of synaptic clusters of the glutamate receptor, the most important excitatory neurotransmitter. Indeed, it has been shown that the blockade or knockdown of the spinal KCC2 in normal rats significantly reduced nociceptive threshold,

confirming that the reported disruption of anion homeostasis in lamina I neurons was sufficient to cause neuropathic pain (Chamma et al., 2012).

Of the two existing potassium-chloride co-transporters, only KCC2, has been associated with PDN (Jolivalt et al., 2008; Lee-Kubli & Calcutt, 2014; Morgado, Pereira-Terra, Cruz, & Tavares, 2011; Morgado, Pereira-Terra, & Tavares, 2011; Morgado, Pinto-Ribeiro, & Tavares, 2008). All of these studies demonstrated that STZ-diabetic rats exhibit a significant decrease in KCC2 expression at the spinal cord and, due to this GABA presented excitatory actions, contributing to spinally-mediated hyperalgesia in diabetes. In particular, Morgado and colleagues (C. Morgado, P. Pereira-Terra, et al., 2011; C. Morgado, P. Pereira-Terra, et al., 2011; Morgado et al., 2008) verified that normalization of KCC2 expression at the spinal cord of STZ-diabetic rats with PDN was shown to reduce spinal hyperactivity and to elicit anti-nociception, pointing for a key role of KCC2 in spinal pain abnormal nociceptive processing during PDN.

3.1.1.2 KCC2 and GABA Connection

GABA is the major inhibitory neurotransmitter involved in spinal pain modulation in the adult nervous system. However, it can also have an excitatory role during embryonic neuronal development and in pathological conditions, such as chronic pain and epilepsy (Cordero-Erausquin, Coull, Boudreau, Rolland, & De Koninck, 2005; Coull et al., 2003). Indeed, the activation of ionotropic post-synaptic GABA A receptors ($GABA_AR$) was shown to have excitatory depolarizing effects in spinal nociceptive neurons in chronic pain, which was shown to be due to a reversal in chloride neuronal flux induced by the downregulation in KCC2. In normal conditions, low intracellular levels of chloride are observed and the activation of $GABA_AR$ induces the influx of chloride into the neuron that results in neuronal hyperpolarization and inhibition of spinal pain transmission (Coull et al., 2003). The opposite

occurs when chloride accumulates in the neuron, which was shown to occur when KCC2 was down-regulated or malfunctioning (Coull et al., 2003; Rivera et al., 1999). In such cases, a shift in GABA role from hyperpolarization to depolarization (Balena, Acton, Koval, & Woodin, 2008; Cordero-Erausquin et al., 2005; Coull et al., 2003; Stil et al., 2009) was observed, promoting excitatory instead inhibitory neuronal effects (Figure 2) (Cordero-Erausquin et al., 2005; Coull et al., 2003; Lavertu, Côté, & De Koninck, 2013; Stil et al., 2009).

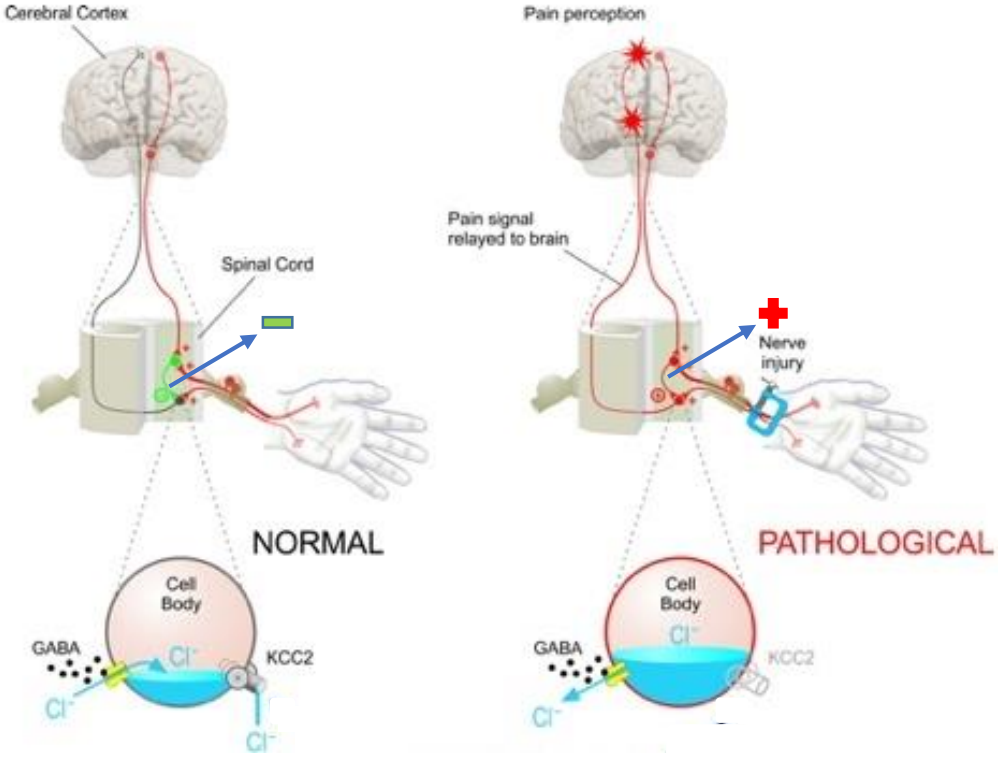

Figure 2 – KCC2 function in normal and pathological conditions. Modified from http://www.painresearchforum.org. Credit: Sylvain Côté, Université Laval.

4. Therapeutic Strategies for Painful Diabetic Neuropathy

Until now, prevention and management of underlying diabetes is the major approach to inhibit the development of painful diabetic neuropathy. The most successful strategy for preventing neuropathy in patients with diabetes is an intensive control of hyperglycemia and lifestyle modifications, increasing physical activity and control of food intake (Skyler, 2004). In fact, there is

no real treatment for PDN but for the symptoms when prevention does not result, as pain relieved drugs, and even those are poorly effective in pain relief during diabetes (Peltier, Goutman, & Callaghan, 2014). Unfortunately, the majority of affected patients do not report pain symptoms until PDN is severe and, in most of the cases, an irreversible condition (Tesfaye et al., 2010). Currently, there are three types of drugs used to relieve the symptoms of PDN: antiepileptics, antidepressants and non-specific analgesics. However, these drugs have been demonstrated to have poor efficacy besides presenting serious side effects such as orthostasis, somnolence, vertigo, urinary retention and erectile dysfunction (Boulton et al., 2005; Peltier et al., 2014; Tesfaye, Vileikyte, Rayman, Sindrup, Perkins, Baconja, Vinik, & Boulton, 2011).

It is, then, extremely important to develop strategies to early diagnose PDN and preventive approaches to avert the pain symptoms. (Duby et al., 2004; Skyler, 2004; Tesfaye et al., 2010).

5. MicroRNAs as Potential Therapeutic Targets in Painful Diabetic Neuropathy

5.1 MicroRNAs Definition

The microRNAs (miRNAs) are a family of small RNAs with approximately 21 to 25 nucleotides and can modulate, negatively, gene expression at the post-transcriptionally level. miRNAs are non-coding RNAs that are derived from larger precursors that form imperfect stem-loop structures. In animals, most miRNAs bind to the target-3′ UTR with imperfect complementarity and function as translational repressors. miRNAs modulate gene expression driving RNA-induced silencing complex (RISC) to the mRNA targets. It can be by: (1) inducing mRNA degradation or (2) inhibiting the translation of target mRNAs. Once incorporated into a cytoplasmic RISC, the miRNA will specify cleavage if the mRNA target has sufficient complementarity to the miRNA, or it will repress productive translation if the

mRNA does not have sufficient complementarity to be cleaved. The small RNAs remains intact after cleavage of the mRNA target and can guide the recognition and destruction of other targets (Bartel, 2004; He & Hannon, 2004; Ruberti, Barbato, & Cogoni, 2012).

The target mRNAs are recognized depending on the complementarities between positions 2 to 8 from the 5′ of miRNA (the seed sequence), and an miRNA Responsive Element (MRE) usually located inside the mRNA 3′ untranslated region (3′ UTR). The knowledge of this mechanism may be applied to target miRNA expression: directly, by using oligonucleotides or virus based constructs, and indirectly, by using drugs to modulate miRNA expression at the transcriptional and/or processing level (Ruberti et al., 2012).

5.2 MicroRNAs in Diabetes

During recent years, there have been increasing studies suggesting that the development of diabetes can result from miRNAs-associated gene expression alterations in several tissues that are critical under diabetes condition (Guay, Roggli, Nesca, Jacovetti, & Regazzi, 2011; Lawrie, 2013; Shantikumar, Caporali, & Emanueli, 2012). More precisely, several miRNAs have been shown to be involved in pancreas and β-cells function, affecting insulin production, its secretion and action (Fernandez-Valverde, Taft, & Mattick, 2011). Several miRNAs have already been studied and found to play a role in the adjacent disorders of diabetes, such as obesity, nephropathy, retinopathy, neuropathy and cardiac disease (Fernandez-Valverde et al., 2011; Kato, Castro, & Natarajan, 2013; Lawrie, 2013; Shantikumar et al., 2012).

Further to the association between miRNAs and diabetes, they have also been shown to relate to the central and peripheral sensitization and chronic pain disorders, such as inflammatory, neuropathic and visceral pain (Andersen, Duroux, & Gazerani, 2014; Kusuda et al., 2011). At the spinal cord level, there are studies using different animal models of

chronic neuropathic pain where up-regulation of few miRNAs is regarded (Brandenburger et al., 2012; Sakai & Suzuki, 2014)

Considering the inhibitory role of miRNAs, and considering the possibility of constructing vectors that silence their actions in specific cells, it is clear that miRNAs may be regarded as potential therapeutic targets in chronic pain conditions such as PDN (Kress et al., 2013; Zhao et al., 2010).

II. Objectives

Considering the role of microRNA-92 (miR-92) in the regulation of KCC2 expression and the impairments reported for this co-transporter in the spinal cord during PDN, it is important to evaluate if miR-92 has a role in PDN-associated KCC2 downregulation, inasmuch as it may represent a potential novel target for pain relief.

This study aims at (1) investigating whether miR-92 plays a role in the regulation of spinal cord KCC2 expression in STZ-diabetic rats with PDN, (2) evaluating the pain-relieving therapeutic potential of silencing miR-92 in the spinal cord of STZ-diabetic rats with PDN, (3) assessing the effects of a KCC2 inhibitor and a $GABA_AR$ antagonist on the mechanical nociception of STZ-diabetic rats after silencing of miR-92, (4) evaluating if inflammatory conditions may interfere with miR-92 and KCC2 neuronal expression.

III. Materials and Methods

1. Animals

Male Wistar rats were purchased from Charles River, France. Rats were initially housed at random in groups of four animals per cage, in a room with controlled environment (temperature, 22 ± 2ºC; humidity, 45-65%; 12-hour light/dark cycle), and received food and water ad libitum. All procedures were performed in accordance with the ethical guidelines of the European Community Council Directive 2010/63/EU, and of the International Association for the Study of Pain for experimental pain research in conscious animal (Zimmermann, 1983).

2. Preparation of Type 1 Diabetes Animal Model

In vivo experiments were performed in the well-established streptozotocin (STZ)-induced Wistar rat model of type 1 diabetes (Courteix, Eschalier, & Lavarenne, 1993; Lenzen, 2008; Szkudelski, 2001). The STZ is a cytotoxic glucose analogue that selectively causes death of pancreatic β-cells, causing an abrupt loss of insulin secretion (Figure 3) (Lenzen, 2008; Szkudelski, 2001).

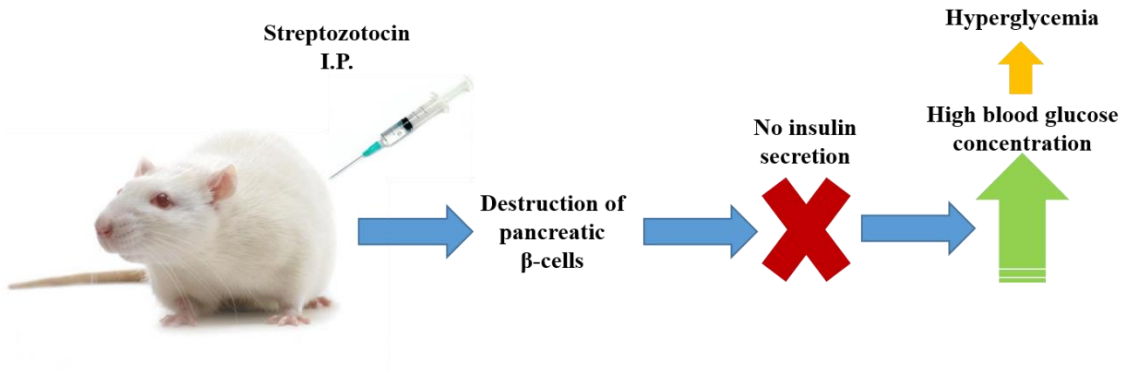

Figure 3 – Mechanism of streptozotocin (STZ) action in the STZ-induced rat model of type 1 diabetes.

Briefly, type 1 diabetes was induced in male Wistar rats (280-300 g) by intraperitoneal (i.p.) injection of STZ (60 mg/g body weight, Sigma-Aldrich, Portugal) dissolved in 0,1 M citrate buffer (pH=4,5). Control animals (CTR) received equal volumes of vehicle solution. After three days, blood glucose concentration was measure in blood samples taken from the tail vein of STZ-injected rats using glucose oxidase-impregnated strip testing (Breeze®, Bayer, Portugal). STZ-injected rats presenting blood glucose concentration higher than 270 mg/dL were considered diabetic (Calcutt, 2004) and included in the study.

3. Behavioral Evaluation

3.1 Mechanical Nociception

Mechanical nociception was evaluated in STZ-diabetic rats by using the Randall-Selitto paw-pressure test (PPT) (Ugo-Basile, Comerio, VA, Italy) (Randall & Selitto, 1957). Animals were handled daily by the experimenter for 7 days prior to the beginning of the tests, for habituation purposes. For the PPT, ascending mechanical forces were applied to the dorsal surface of right hindpaw and the mechanical force (in grams) that induced hindpaw withdrawal was recorded. The paw withdrawal threshold (PWT) of each animal was calculated as the average of three consecutive measurements, taken at 2 min intervals.

3.2 Locomotor Activity

Locomotor activity levels were assessed by performing the open field test (OFT). Each rats was individually placed in the center of a black acrylic open field arena (45x45x45 cm) and filmed for 10 minutes (min). The total distance travelled (in cm) by each rat was quantified using the Smart software version 3.0 (Panlab Harvard Apparatus).

4. Lentiviral Vectors Preparation

All construction and preparation of miRNA sponge vectors were made at the Institute of Cell Biology and Neurobiology, National Research Council (Rome, Italy), as described elsewhere (Barbato et al., 2010). To produce lentiviral particles, a third generation lentiviral vector and three plasmids were used. Each plasmid construct expresses important gene for lentiviral production. The mixture of these four plasmids was transfected in Human Embryonic Kidney (HEK) 293T cells. HEK293T cells virus-containing-medium was harvested 60 hours after transfection filtered and concentrated by ultracentrifugation. The titers of the viral vectors were in the range of 1-3 $\times$ 10^9 TU/mL (TU: transducing units) (Dull et al., 1998; Vilardo, Barbato, Ciotti, Cogoni, & Ruberti, 2010).

In order to inhibit miR-92, the sponge lentiviral vector, pLSyn-miR-92 sponge, contains four binding sites to sequester miR-92 (Figure 4). pLSyn vector without binding sites for miR-92 was used as control (Figure 5). Both lentivirus constructs contain the enhanced green fluorescent protein (EGFP) gene under the control of the synapsyn promoter that allows the expression only in neuronal cells (Barbato et al., 2010). The expression of EGFP allows the quantification of transfection and transcription of lentiviral particles transgenes.

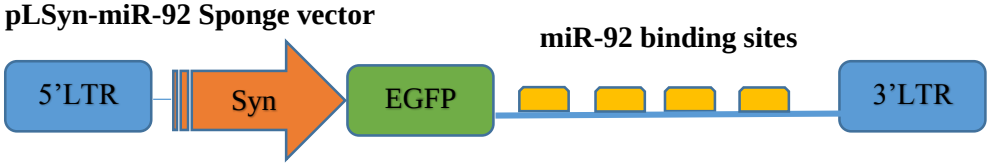

Figure 4 – Illustration of pLSyn-miR-92 Sponge vector construct. 5'LTR: long terminal repeat on 5' end (initiation). Syn: synapsyn promotor. EGFP: enhanced green fluorescence protein. 3'LTR: long terminal repeat on 3' end (3' end formation of viral transcripts).

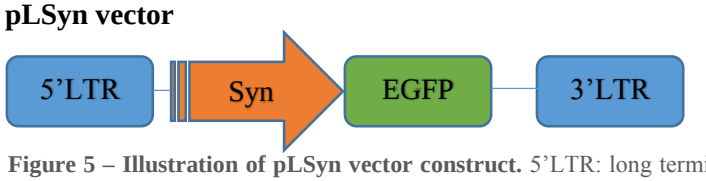

Figure 5 – Illustration of pLSyn vector construct. 5'LTR: long terminal repeat on 5' end (initiation). Syn: synapsyn promotor. EGFP: enhanced green fluorescence protein. 3'LTR: long terminal repeat on 3' end (3' end formation of viral transcripts).

5. Intraspinal Lentiviral Inoculations

For all inoculation procedures, rats were firstly anaesthetized with an i.p. injection of a mixture of ketamine and medetomidine (5 mg/kg of ketamine and 1 mg/kg of medetomidine), and anesthesia was then maintained with isoflurane (1-1.5% in 60% oxygen/air mixture) (Figure 6A). A dorsal laminectomy of spinal vertebrae T13-L1 was performed (Figure 6B). The dura mater was slit and two pressure injections, of 1.5 μL each, were bilaterally performed about 1 mm lateral to the dorsal vertebral artery and 0.5 mm in depth through spinal cord surface, using a 10 μL Hamilton syringe coupled to a glass micropipette with a tip diameter of about 30-40 µm. Injections were performed slowly at 2-min intervals between each 0.1 μL bolus, and a 10-min waiting period was allowed after total volume injection to avoid reflux. Afterwards, the incision was closed with suture and atipamezole hydrochloride (1 mg/kg) was administered by an intra-muscular injection in order to reverse anesthesia. Animals were monitored for 4-5 hours after surgery and treated orally with tramadol hydrochloride (10 mg/kg) during that period. Animals were housed one per cage to prevent wound damage.

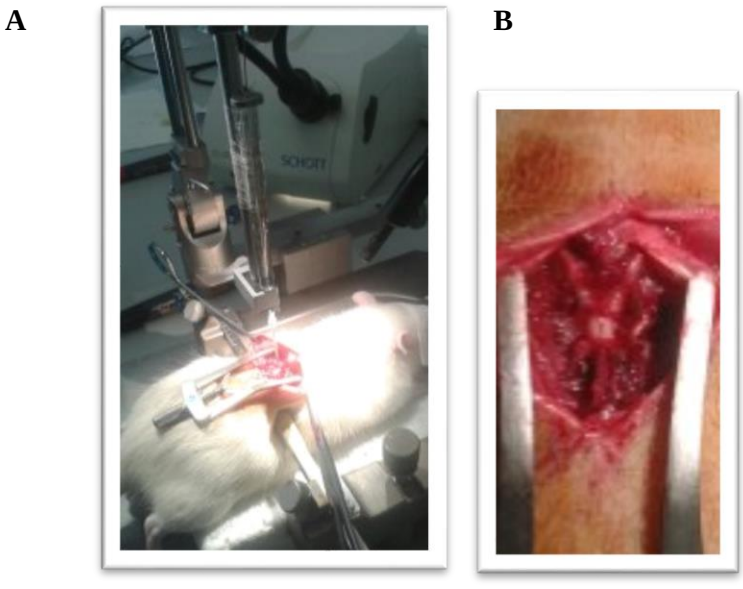

Figure 6 – Intraspinal lentiviral inoculation. (A) Stereotactic surgical apparatus adapted for intraspinal injection. **(B)** L4-L5 spinal cord segment.

6. Intrathecal Drug Administration

Intrathecal administrations of a KCC2 specific inhibitor—[(dihydroindenyl)oxy] Alkanoic acid (DIOA), 30 µg (Sigma-Aldrich), a $GABA_AR$ antagonist—Bicuculline (BIC), 0.6 µg (Sigma-Aldrich), or vehicle solution [saline + 10% DMSO (dymetil sulfoxide)] were performed as follows. Each administration was carried out at least 48h apart to assure a suitable washout of the previous injected drug. Intrathecal injections (30 µl) were performed with a 26-gauge needle coupled to a 100 µl Hamilton syringe by spinal puncture of intervertebral space at L5-L6 or L6-S1 level (Figure 7) under volatile anesthesia (2.5-5% isoflurane in 100% oxygen). This methodology was adapted from Jolivalt et al. (Jolivalt et al., 2008).

Figure 7 – Illustration of the intrathecal site of drug administration. Modified from http://paperheartrats.com/blog/

7. Animals Culling and Spinal Cord Tissue Collection

At the end of the *in vivo* experiments, rats were anesthetized with pentobarbital sodium (i.p. 50 mg/g body weight) and then decapitated. The spinal cord segments L4-L5 were promptly dissected and stored at -80ºC until further analyses.

8. Primary Neuronal Cell Cultures

All experiments using neuronal cultures were performed at the Institute of Cell Biology and Neurobiology, National Research Council (Rome, Italy). In order to evaluate the role of TNF-α and IL-1β in neuronal expression of KCC2 and miR-92, primary neuronal cultures were prepared from hippocampal and spinal cord neurons harvested from Wistar rat embryos on embryonic days 17-18 (E17-18). The tissues were dissected in HEPES-buffered Hanks' balanced salt solution (Gibco) and dissociated via trypsin/EDTA treatment. Cells were plated at 1×10^6 cells on 3.5-cm dishes pre-coated with poly(D/L-lysine) and cultured in neurobasal medium supplemented with B-27 and glutaMAX (Gibco), which was changed every 3–4 days (Barbato et al., 2010).

To evaluate the role of TNF-α and IL-1β in neuronal expression of KCC2 and miR-92, primary hippocampal and spinal neurons after 15 days in culture, were treated with 50 ng/mL rat TNF-α (Sigma-Aldrich) or 10 ng/mL rat IL-1β (Sigma-Aldrich). 24h after treatment, neurons were harvested and used for Western blotting and RT-PCR analyses.

9. Western Blotting

9.1 Primary Neuronal Cell Cultures

Hippocampal and spinal cord neurons were scrapped and homogenized in lysis buffer (1% Triton X-100, 0,25% SDS, 1% Sodium Deoxycholate, 2mM EDTA, 1mM DTT). After several freeze/thaw cycles and centrifugation at 12000xg for 20 min at 4ºC, supernatants were incubated 30 min on ice. Total protein concentration was quantified by detergent compatible (DC) protein assay (BioRad, Italy) using Bovine Serum Albumin (BSA) as a standard. For this experiment, the membranes were blocked in 7% skim milk in TBS-T (Tris

buffered saline with 0,05% Tween) for 1 hour at room temperature and then incubated in primary antibody rabbit anti-KCC2 (1:1000) in TBS-T containing 7% skim milk for 24 hours at 4ºC. GAPDH (Glyceraldehyde-3-phosphate dehydrogenase) was used as internal control, the membrane was blocked in 5% skim milk in TBS-T for 1 hour at room temperature and then incubated in primary antibody mouse anti-GAPDH (1:6000) in TBS-T containing 2% of skim milk. The membranes were then carefully washed with TBS-T and incubated with secondary antibody conjugated to horseradish peroxidase (HRP).

9.2 Spinal Cord Samples

The expressions of KCC2 and enhanced green fluorescent protein (EGFP) in the spinal cords from rats inoculated with pLSyn and pLSyn-miR-92 sponge lentiviral particles were determined by Western blotting analysis. Freshly dissected spinal cord L4-L5 segments were homogenized with a tissue homogeniser in lysis buffer (MOPS 20mM; EGTA 2mM; EDTA 5mM; 1% Triton X-100) containing proteases inhibitor (1:100, Sigma-Aldrich, St. Louis, MO) and phosphatase inhibitor cocktail 2 and 3 (1:100, Sigma- Aldrich, St. Louis, MO). The homogenates were incubated on ice for 20 min and then centrifuged for 20 min at 21100xg at 4ºC. The supernatants were collected and centrifuged again for 10 min at 21100xg at 4ºC. Total protein concentration in the final supernatants was quantified by the Bradford method using BSA (Nzytech, Portugal) as a standard. Protein samples (40 µg) were added to 4x sample buffer (240 mM Tris/HCl pH 6.8, 40% glycerol, 8% SDS, 0,04% bromophenol blue) containing 10% of β-mercaptoethanol and denatured at 100ºC for 5 min. The samples and molecular weight marker (Protein Marker VI-10-245, AppliChem, USA) were loaded on a 8% polyacrylamide gel and subjected to Sodium Dodecyl Sulfate-Polyacrylamide Gel Electrophoresis (SDS-PAGE) at 20 mV, followed by electroblotting to a nitrocellulose membrane at 30 mV overnight. The membranes blots were then washed twice with phosphate buffered saline (PBS) containing 25% Triton X-100—PBS-T— and immersed in

Ponceau S Red staining solution (0.2 % Ponceau, 3% trichloroacetic acid and 3% sulphosalicylic acid) for 5 min to confirm protein transfer. After gently washing with distilled water, blots were immediately photographed using the Chemidoc system (BioRad, Portugal). Blots were then abundantly washed with PBS-T and, immersed in a blocking solution containing 5% skim milk in PBS-T for 1 hour at room temperature. Following this, blots were incubated with the appropriate primary antibody—rabbit anti-KCC2 (1:2000) or rabbit anti-GFP (1:2000) in PBS-T containing 5% BSA— for 24 hours at 4 ºC. On the following day, blots were carefully washed in PBS-T and incubated with anti-rabbit secondary antibody conjugated to horseradish peroxidase (HRP) (1:10000, GE Healthcare, USA) in PBS-T with 5% of skim milk for 1 hour. After washing with PBS-T, blots were incubated with Clarity Western ECL Substrate (BioRad, Portugal) for 5 min and immunoreactive bands were detected by Chemidoc system (BioRad, Portugal).

α-tubulin was used as an internal loading control, being the blots incubated with an anti-α-tubulin primary antibody raised in mouse (1:10000, Sigma-Aldrich, St. Louis, MO) followed by incubation in anti-mouse secondary antibody conjugated to HRP (1:10000,GE Healthcare, USA). Detection and quantification of α-tubulin immunoreactive bands were performed as described above. Western blotting analyses results for each sample were calculated as the densitometric units ratio between the protein of interest and α-tubulin, and presented in arbitrary units.

10. Real-Time PCR

Total RNA was extracted from either spinal cord tissue L4-L5 segments or hippocampal and spinal cord primary culture neurons, using TRIzol (Invitrogen) reagent according to the manufacturer's instructions. Then, RNA was treated with TURBO DNA-free kit (Ambion) to avoid any possibility of DNA contamination. RNA quantification was performed by spectrophotometric analysis using the NanoDrop 2000 (Thermo Scientific).

For miR-92 quantification, the extracts were reverse-transcribed using Taqman microRNA reverse transcription kit (Applied Biosystems), and amplified with FastStart Universal Probe Master (Roche) in a 7900HT Fast Real-Time PCR System (Applied Biosystems). Relative changes in gene expression were quantified using the comparative threshold method (Ct) after determining the Ct values for endogenous control U6 and target miR-92 in each sample set. The experiments were performed using triplicates for each sample.

For KCC2 mRNA, cDNA was synthetized using SuperScript III Reverse Transcriptase (Invitrogen, Italy) and amplified with the SensiMixPlus SYBR Kit (BioLine, Italy). Rat TATA binding (TBP) and KCC2 were amplified using the oligonucleotides for *Rattus norvegicus:* (RNO): RNO-TBP-RW:CAATTCTGGGTTTGATCATTCTG; RNO-TBP-FW:CCCACCGCAGTTCAGTAGC; RNO-KCC2-FW:CCTCTTTCTGCGGCTCACT; RNO-KCC2-RW: GAAATGGCTGTGAGCATCG (Barbato et al., 2010; Vilardo et al., 2010). Relative changes in gene expression were quantified using the comparative threshold method described above.

11. Statistical Analysis

GraphPad Prism version 6.0 was used for statistical analyses. The results from KCC2 mRNA and miR-92 expression levels were compared by independent sample t test. Blood glucose concentration and body weights of STZ rats were compared by independent sample t test. The PWTs from STZ rats treated with pLSyn and pLSyn-miR-92 sponge were compared by Two Way Analysis of Variance with repeated measures (ANOVA-RM) followed by Bonferroni post-hoc test for multiple comparison. The behavioral findings from the time-course pharmacological study performed in STZ-inoculated rats were compared by ANOVA-RM followed by Bonferroni post-hoc test for multiple comparisons. In this analysis, one STZ rat inoculated with pLSyn and receiving BIC was excluded from the statistical analysis because the execution of PPT was not performed at 15 min as the animal was still under anesthesia and without normal reflexes. The western blot results from

STZ-inoculated animals were compared by independent sample t test. Results from cell experiments were compared by One-Way ANOVA followed by Bonferroni post-hoc test for multiple comparisons. Results are presented as mean±SEM and statistical significance was settled at $p<0.05$.

IV. Results

1. Study 1: Evaluation of the expression levels of KCC2 mRNA and miR-92 in the spinal cord of STZ-induced type 1 diabetic rats with PDN

A key role for KCC2 in spinal abnormal pain processing during PDN has been suggested in different studies (Jolivalt et al., 2008; Lee-Kubli & Calcutt, 2014; C. Morgado, P. Pereira-Terra, et al., 2011; C. Morgado, P. Pereira-Terra, et al., 2011; Morgado et al., 2008). Although all of these studies have reported decreased levels of KCC2 in the spinal cord of STZ-diabetic rats with PDN compared to healthy animals, the mechanisms behind it are still elusive. However, *in vitro* studies using primary cultures of cerebellar granule (Barbato et al., 2010) and hippocampal (Vetere et al., 2014) neurons from healthy rodents demonstrated an inverse relationship between the levels of KCC2 and miR-92. We, therefore, hypothesized that the decrease in the levels of KCC2 observed in the spinal cord of STZ-diabetic rats with PDN could be mediated by increases in the levels of miR-92. In order to test our hypothesis, we evaluated the levels of miR-92 and KCC2 mRNA in L4-L5 spinal cord samples from healthy and STZ-diabetic rats by RT-PCR analysis (Figure 8).

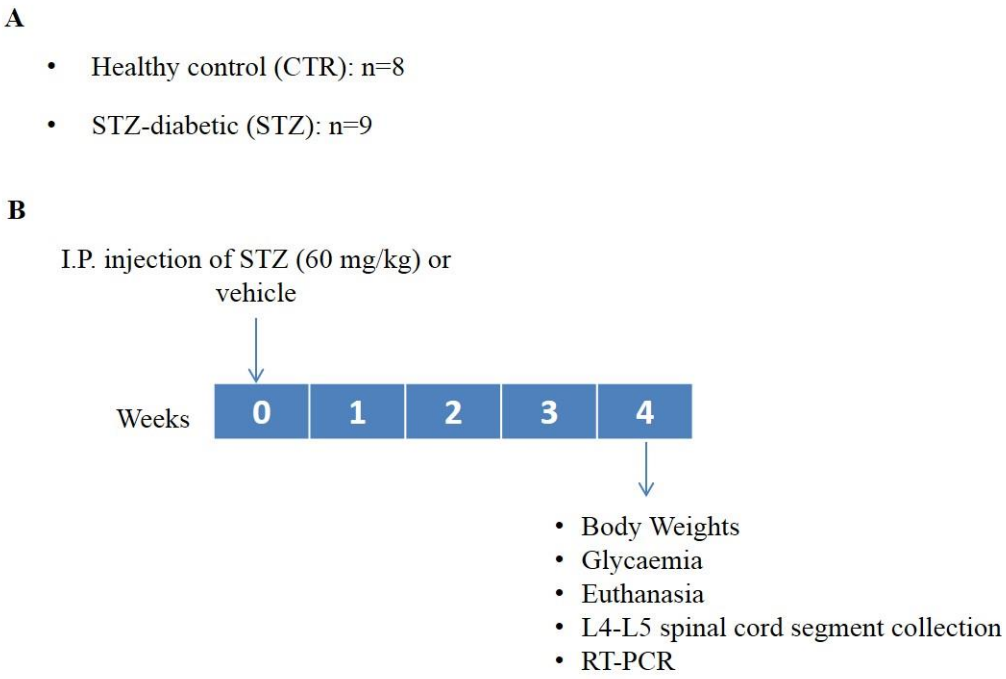

Figure 8 – Experimental design of Study 1: Evaluation of the expression levels of KCC2 mRNA and miR-92 in the spinal cord of STZ-induced type 1 diabetic rats with PDN. (A) Experimental groups. **(B)** Timeline.

1.1 Study 1 Results

1.1.1 Blood glucose concentration and body weights

In order to monitor metabolic parameters characteristic of this rat model of type 1 diabetes, glycaemia and body weights were assessed 4 weeks after STZ injection. We verified that STZ-diabetic rats presented increased blood glucose levels and decreased body weight compared to control animals (Figures 9 and 10, respectively).

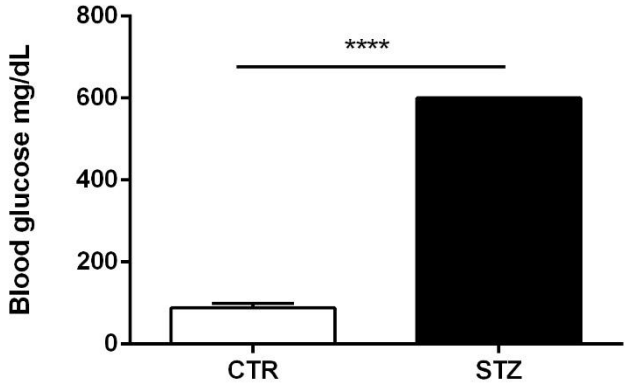

Figure 9 – Blood glucose levels of STZ-induced diabetic rats. Average blood glucose levels of control (CTR) (n= 8) and STZ-diabetic (STZ) (n= 9) rats 4 weeks after diabetes induction. Error bars represent SEM.Unpaired t test, ****p<0,0001.

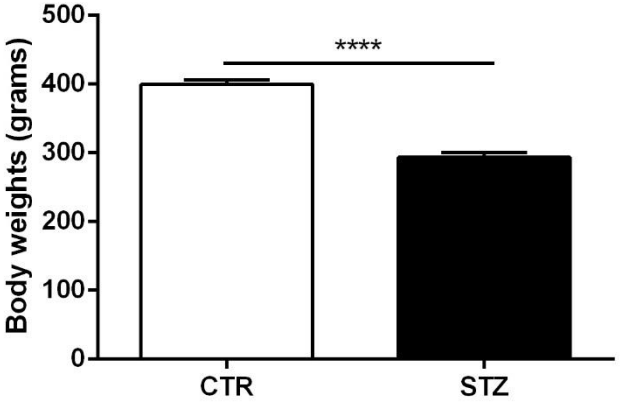

Figure 10 – Effect of STZ-induced diabetes on body weight. Average body weights of control (CTR) (n= 8) and STZ-diabetic (STZ) (n= 9) rats 4 weeks after diabetes induction. Error bars represent SEM. Unpaired t test, ****p<0,0001.

1.1.2 Spinal cord miR-92 and KCC2 mRNA expression levels

For miR-92 expression levels analysis, two RT-PCRs were independently made, each using different STZ-diabetic and CTR animals. Both assays revealed significant increased

expression of miR-92 in the spinal cord of STZ-diabetic rats when compared with healthy control animals (Figure 11)

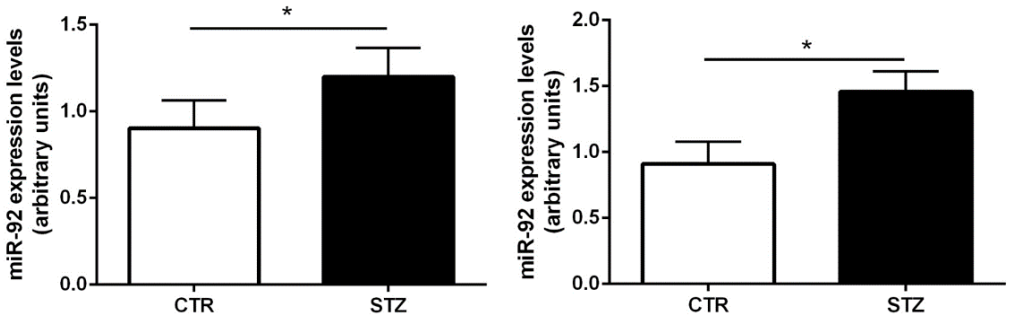

Figure 11 – Effect of STZ-induced diabetes on spinal cord miR-92 expression levels. RT-PCR quantification of miR-92 expression levels in the L4-L5 spinal cord segment of control (CTR) and STZ-diabetic (STZ) rats. On the left graph, the results of the first experiment using four CTR and four STZ animals are shown. On the right graph, the results of the second experiment using further four CTR and four STZ animals are shown. Error bars represent SEM. Unpaired t test, *p<0,05.

The levels of KCC2 mRNA expression were analyzed and compared in L4-L5 spinal cord segments of CTR and STZ-diabetic rats. No changes in KCC2 mRNA expression levels were detected between both groups of animals (Figure 12).

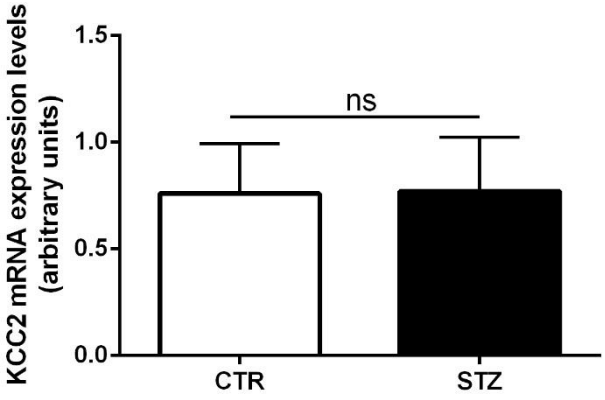

Figure 12 – Effect of STZ-induced diabetes on the spinal cord KCC2 mRNA expression levels. RT-PCR quantification of KCC2 mRNA expression in the L4-L5 spinal cord segment of control (CTR) (n=4) and STZ-diabetic (STZ) (n=4) group. Error bars represent SEM. Unpaired t test, non-significant (ns).

Our results suggest that increased levels of miR-92 in the spinal cord of STZ-diabetic rats with PDN may, indeed, mediate the decreases in KCC2 (at the protein level) observed in these animals (C. Morgado, P. Pereira-Terra, et al., 2011; C. Morgado, P. Pereira-Terra, et al., 2011; Morgado et al., 2008).

2. Study 2: Evaluation of the therapeutic potential of the selective inhibition of miR-92 in the spinal cord of STZ-induced type 1 diabetic rats with PDN

Given the results of Study 1, supporting a possible role for miR-92 in PDN through spinal cord KCC2 levels modulation, we considered important to evaluate the therapeutic potential of a selective inhibition of miR-92 in this condition. Our approach was based on that of a recent study in mice by Vetere and colleagues (Vetere et al., 2014) in which the selective inhibition of miR-92, using a mir-92 sponge lentiviral vector, was shown to prevent decreases in KCC2 hippocampal expression and alter memory formation process. Briefly, we intraspinally administered a lentiviral vector to restrain miR-92—pLSyn miR-92 sponge—to STZ-diabetic rats, while STZ-diabetic sham controls were administered pLSyn vector only. To evaluate whether inhibition of miR-92 is able to modulate the mechanical hypersensitivity exhibited by this animal model of type 1 diabetes (Morgado et al., 2008; Morgado, Silva, Pereira-Terra, & Tavares, 2011) through increases in spinal cord KCC2 levels, all animals were behaviorally evaluated for mechanical nociception using the Randall-Selitto test and the levels of KCC2 in their spinal cords were analyzed by Western blotting (Figure 13).

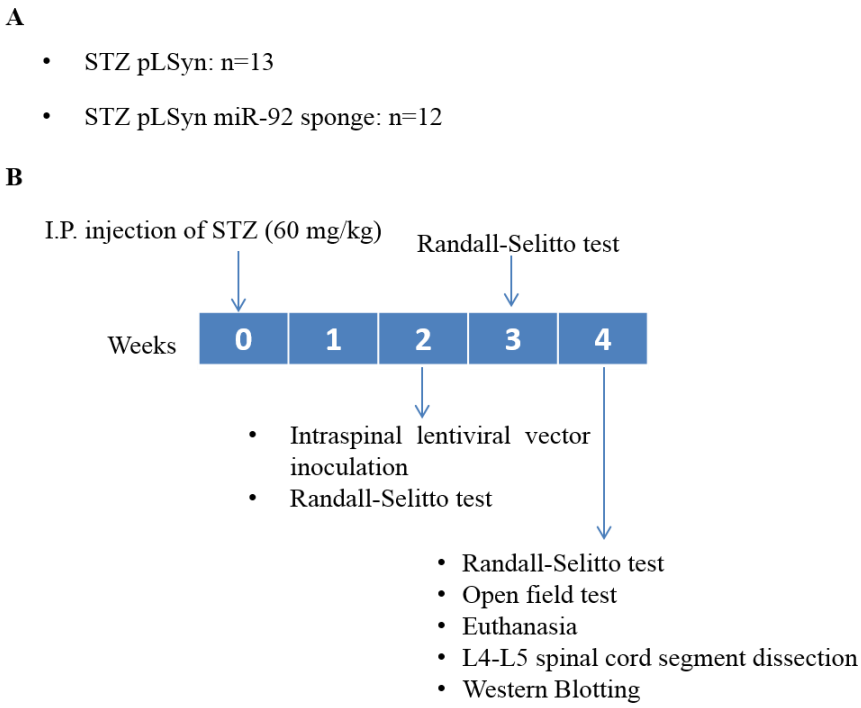

Figure 13 – Experimental design of Study 2: Evaluation of the therapeutic potential of the selective inhibition of miR-92 in the spinal cord of STZ-induced type 1 diabetic rats with PDN. (A) Experimental groups. **(B)** Timeline.

2.1 Results

2.1.1 Blood glucose concentration and body weights

As in Study 1, all animals were monitored and assessed for glycaemia and body weights during the experiment. At day fourteen after lentiviral particles inoculation, STZ-diabetic rats presented high blood glucose concentration, which did not differ between STZ-diabetic rats inoculated with pLSyn or pLSyn-miR-92 sponge lentiviral particles (Figure 14). Similarly, body weights were not significantly different between both groups (Figure 15).

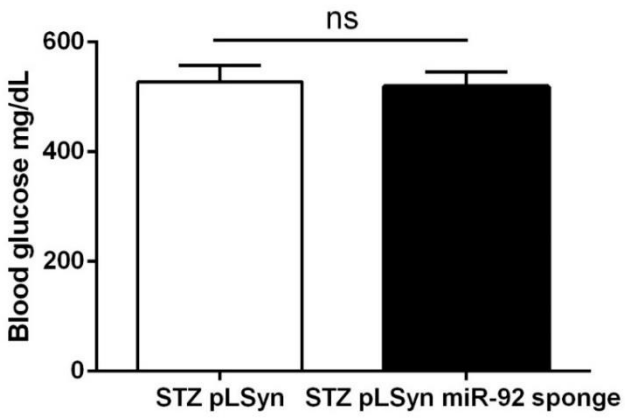

Figure 14 – Blood glucose levels of STZ-diabetic rats after intraspinal lentiviral particles inoculation. Average blood glucose levels of STZ pLSyn (n=13) and STZ pLSyn miR-92 sponge (n=12) rats at 14 days after intraspinal inoculations. Error bars represent SEM. Unpaired t test, non-significant (ns).

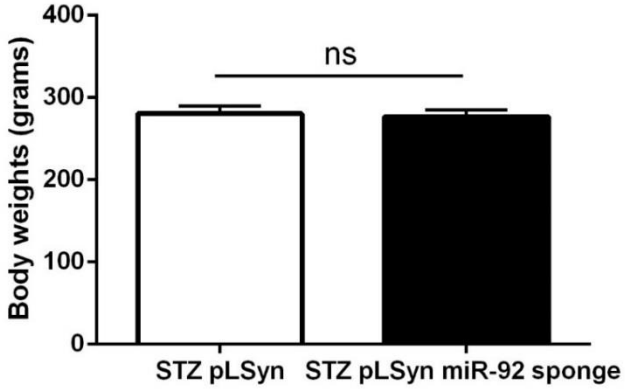

Figure 15 – Body weights of STZ-diabetic rats after intraspinal lentiviral particles inoculation. Average body weights of STZ pLSyn (n= 13) and STZ-pLSyn miR-92 sponge (n= 12) rats 14 days after intraspinal inoculations. Error bars represent SEM. Unpaired t test, non-significant (ns).

2.1.2 Mechanical nociception of STZ rats intraspinally inoculated with pLSyn and pLSyn-miR-92 sponge lentiviral particles

Mechanical nociception was evaluated using the Randall-Selitto paw-pressure test (PPT) in STZ-diabetic rats before (2 weeks post-STZ injection), and 7 and 14 days after pLSyn or pLSyn-miR-92 sponge lentiviral particles intraspinal inoculation.

Two weeks after the induction of diabetes (before the inoculation of the lentiviral particles), our STZ-diabetic rats presented PWT values that are similar to those reported for this rat model of type 1 diabetes upon the development of diabetes-induced hyperalgesia (Carla Morgado et al., 2011). Fourteen days (14D) after the inoculation of pLSyn miR-92 sponge, STZ-diabetic animals exhibited a significant increase in the PWTs compared with the PWTs observed in the pre-inoculation test. Regarding STZ-diabetic rats inoculated only with pLSyn, we observed a decrease in their PWTs after lentiviral particles inoculation compared with the PWTs obtained pre-inoculation, although the results did not reach statistical significance. Further, STZ rats inoculated with pLSyn-miR-92 sponge presented increased PWTs both at day seven (7D) and at day fourteen (14D) after inoculation when compared with STZ rats inoculated with pLSyn only. At day fourteen, the difference in mechanical nociception between the two groups was more pronounced (Figure 16).

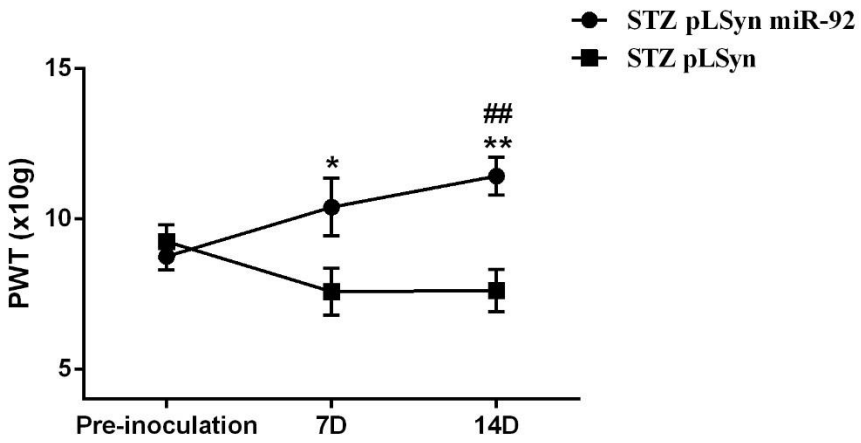

Figure 16 – Effect of intraspinal inoculation of pLSyn control and pLSyn miR-92 sponge lentiviral particles on the mechanical nociception of STZ-diabetic rats with PDN. Paw withdrawal thresholds (PWTs) of STZ-diabetic rats before (Pre-inoculation) 2 weeks after diabetes induction (Pre-inoculation)—at week 2 of diabetes, and 7 (7D) and 14 days (14 D) after intraspinal inoculation of pLSyn (n=10) control lentiviral particles and pLSyn miR-92 (n=11) lentiviral particles evaluated by the Randall-Selitto paw pressure test. Error bars represent SEM. Two-Way ANOVA repeated measures, * corresponds to the comparison between STZ pLSyn miR-92 and STZ pLSyn, *p<0,05, **p<0,01, # corresponds to the comparison between STZ-pLSyn miR-92 sponge with respective pre-inoculation, ## p<0,01.

2.1.3 Locomotor activity of STZ rats intraspinally inoculated with pLSyn and pLSyn miR-92 sponge lentiviral particles

The Open Field test (OFT) was used for the evaluation of locomotor activity of STZ spinally inoculated rats in order to assess whether locomotion was affected by the surgery. This evaluation is critical since possible locomotion disturbances caused by the intraspinal injection procedure can bias the results of the mechanical nociception test. No significant differences were detected between the STZ rats inoculated with pLSyn or pLSyn-miR-92 sponge lentiviral particles (Figure 17).

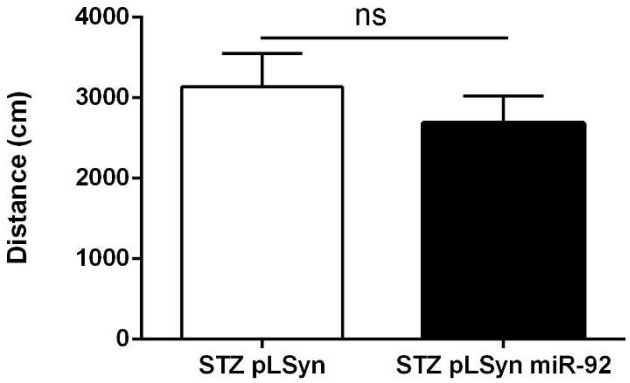

Figure 17 – Analysis of locomotor activity of inoculated STZ-diabetic rats after intraspinal surgery. OFT analysis at 14 days after intraspinal injection of STZ pLSyn (n=10) and STZ pLSyn miR-92 sponge (n=11). Travelled distance in cm was calculated. Error bars represent SEM. Unpaired t test, non-significant (ns).

2.1.4 Spinal cord EGFP protein expression levels

All inoculated animals expressed EGFP as detected by Western blotting, showing that spinal neurons were transfected by lentiviral particles and the contained transgene was transcribed. No significant differences were detected in EGFP expression between the two groups of animals (Figure 18).

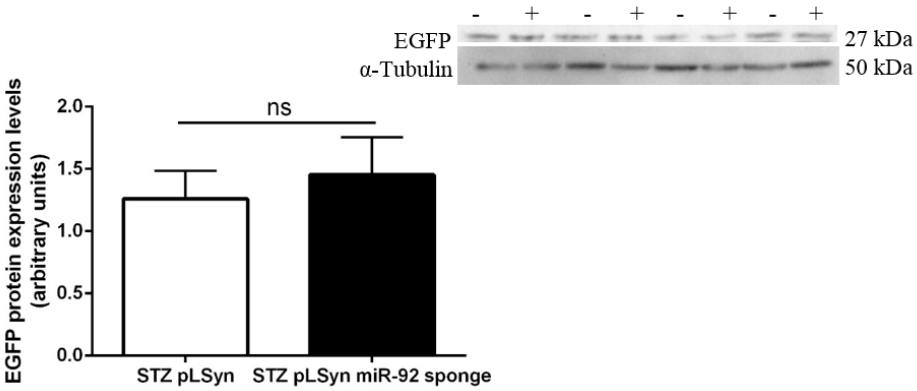

Figure 18 – Quantification of EGFP expressed in the spinal cord of STZ-diabetic rats inoculated with pLSyn and pLSyn miR-2 sponge lentiviral particles. Expression levels of EGFP of STZ pLSyn (n=4) and STZ pLSyn miR-92 sponge (n=4) by Western blotting. Error bars represent SEM. Unpaired t test, non-significant (ns). -, STZ pLSyn, +, STZ pLSyn miR-92 sponge.

2.1.5 Spinal cord KCC2 protein expression levels

To verify whether decreased mechanical sensitivity exhibited by STZ-diabetic rats administered pLSyn miR-92 sponge lentiviral vector as compared to their counterparts that were administered pLSyn was accompanied by increased spinal cord KCC2 levels, the expression of this co-transporter was quantified in L4-L5 spinal cord segments by Western blotting analysis. The results show that spinal cord of KCC2 protein levels were increased in STZ rats that receive an intraspinal inoculation of pLSyn-miR-92 sponge lentiviral particles when compared with STZ rats inoculated with pLSyn (Figure 19).

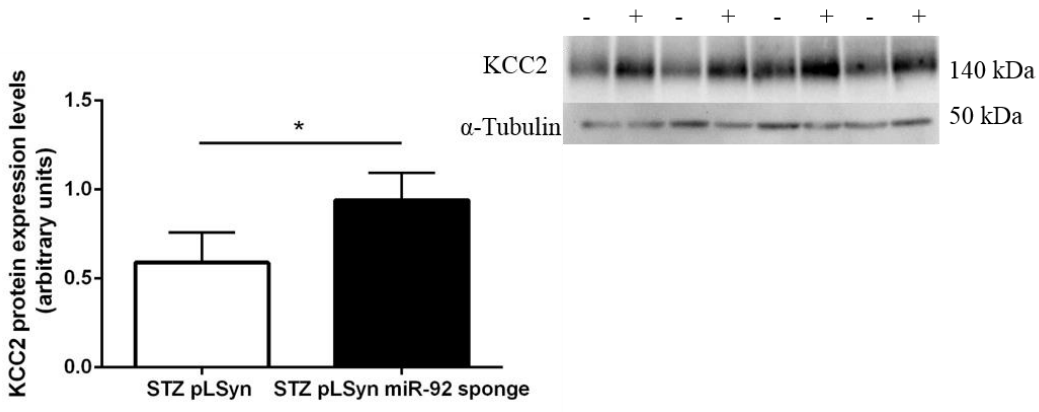

Figure 19 – Effect of viral inoculations on spinal cord KCC2 protein expression levels of STZ-diabetic rats. Expression levels of KCC2 in the spinal cord of STZ pLSyn (n=4) and STZ pLSyn miR-92 sponge (n=4) by Western Blotting. Error bars represent SEM. Unpaired t test, *p<0,05. -, STZ pLSyn, +, STZ pLSyn miR-92 sponge.

In summary, the results of this study show that in a rat model of STZ-induced type 1 diabetes with PDN, STZ-diabetic animals subjected to selective inhibition of spinal cord miR-92 through intraspinal injection of a miR-92 sponge lentiviral vector exhibited increased levels of spinal cord KCC2 protein and decreased mechanical nociception when compared to STZ animals subjected to intraspinal of a control lentiviral vector. Therefore, our results suggest that this procedure of selectively inhibiting spinal cord miR-92 may be regarded as a potential therapeutic strategy in PDN.

3. Study 3: Assessment of the effects of a KCC2 inhibitor and a $GABA_AR$ antagonist on mechanical nociception of STZ-diabetic rats inoculated with pLSyn miR-92 sponge lentiviral particles

To confirm the role of KCC2 as a mediator of the actions of miR-92 inhibition in the analgesia observed in STZ-diabetic rats inoculated with pLSyn miR-92 sponge, and to exclude other possible underlying mechanisms, a proof of concept pharmacological experiment was undertaken by blocking KCC2 with an intrathecal injection of a specific inhibitor, DIOA (30µg) (Jolivalt et al., 2008). Furthermore, given that GABA has been shown to have an excitatory role when KCC2 is down-regulated and, therefore, to play an important role in pain modulation (Chamma et al., 2012; Cordero-Erausquin et al., 2005; Coull et al., 2003; Stil et al., 2009), we decided to evaluate the role of GABA also as possible mediator of the actions of miR-92 inhibition in the decreased nociception observed in STZ.diabetic rats inoculated with pLSyn miR-92 sponge. For this evaluation, a pharmacological study was undertaken by intrathecally injecting these animals with a $GABA_A$ receptor antagonist (which competes with GABA by binding A receptors), bicuculline, (BIC) (0,6µg). Briefly, as illustrated in Figure 20 and following a methodology based on that described by Jolivalt et al (Jolivalt et al., 2008), three weeks after STZ-diabetic rats were inoculated with either pLSyn and pLSyn miR-92, they received an intrathecal injection of DIOA, BIC, or vehicle solution (saline + 10% DMSO) and, after anesthesia recovery, mechanical nociception was evaluated in all animals using the Randall-Selitto PPT 15, 30, 45 and 60 min post-intrathecal administrations. The PWTs were determined as the average of 3 consecutive measures taken at 2-min intervals. In order to minimize the number of experimental animals used in this experiment, and given the preliminary nature of the study, each animal was intrathecally injected 2 or 3 times with DIOA, BIC, or vehicle, being allowed an interval of at least 48h between injections to assure a suitable washout of the previous injected drug (Table 1).

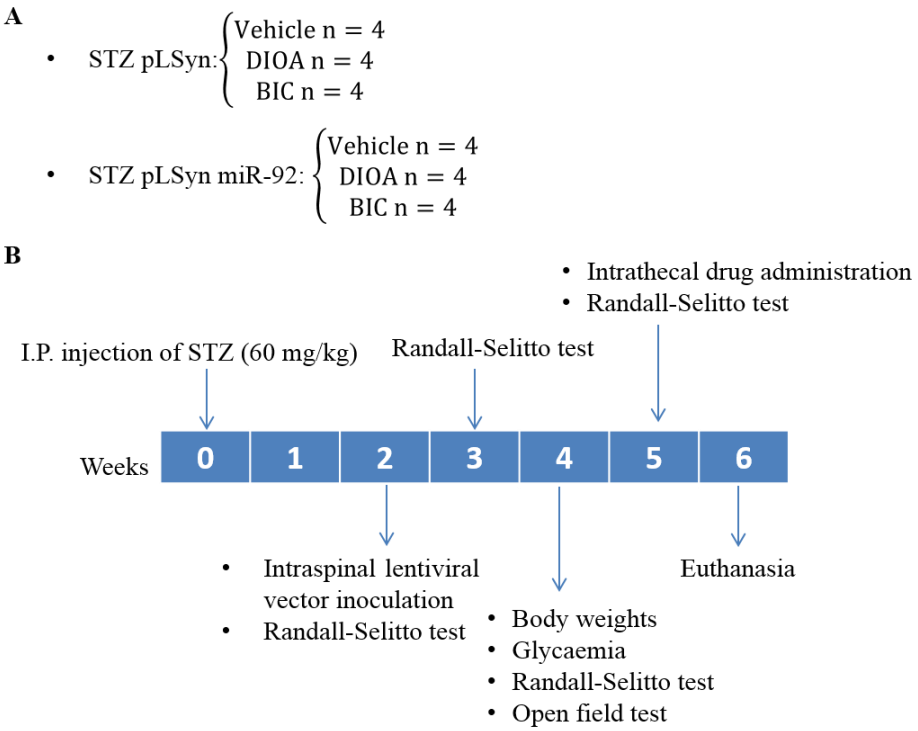

Figure 20 – Experimental design of Study 3: Assessment of the effects of a KCC2 inhibitor and a $GABA_AR$ antagonist on mechanical nociception of STZ-diabetic rats inoculated with pLSyn miR-92 sponge lentiviral particles. (A) Experimental groups. **(B)** Timeline.

Table 1 - Scheme of intrathecal injections on each animal.

		Injection Day				
Animal Group	**Animal number**	**day 1**	**day 2**	**day 3**	**day 4**	**day 7**
STZ pLSyn	6		Vehicle		DIOA	
	9		DIOA		BIC	
	12		DIOA		BIC	Vehicle
	19		BIC		Vehicle	
	20	DIOA		Vehicle		BIC
STZ pLSyn miR-92 sponge	22		Vehicle		DIOA	
	24		DIOA		BIC	
	23		DIOA		BIC	Vehicle
	28	BIC		Vehicle		
	26	DIOA		Vehicle		BIC

Vehicle: Saline + 10%DMSO; **BIC**: Bicuculline; **DIOA**: [(dihydroindenyl)oxy]

3.1 Study 3 Results

3.1.1 Blood glucose concentration and body weights

As in Study 2, all animals presented high blood glucose concentration, which did not differ between STZ rats inoculated with pLSyn or pLSyn-miR-92 sponge lentiviral particles (Figure 21). Also, body weights were not significantly different between both groups (Figure 22).

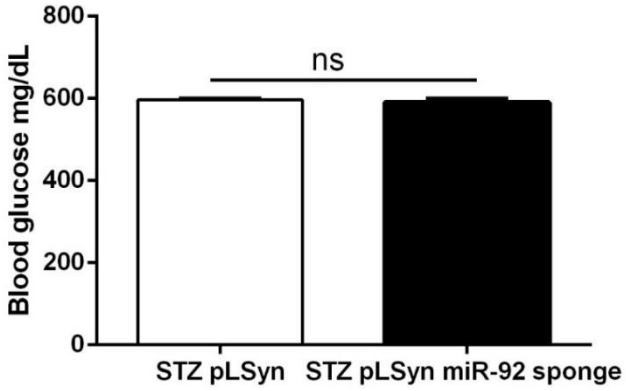

Figure 21 – Blood glucose levels of STZ-diabetic rats after intraspinal lentiviral particles inoculation. Average blood glucose levels of STZ pLSyn (n=6) and STZ pLSyn miR-92 sponge (n=7) rats 14 days after intraspinal inoculations. Error bars represent SEM. Unpaired t test, non-significant (ns).

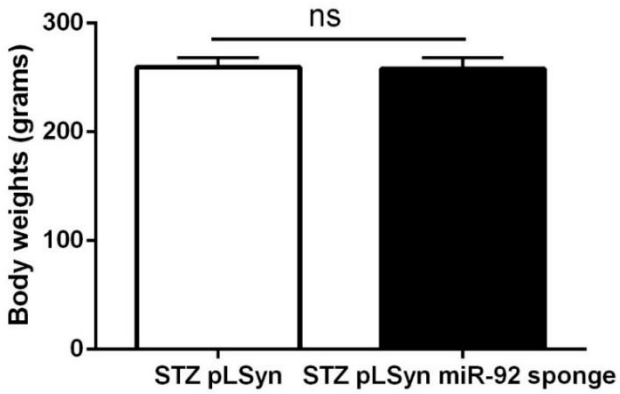

Figure 22 – Body weights of STZ-diabetic rats after intraspinal lentiviral particles inoculation. Average body weights of STZ pLSyn (n= 6) and STZ-pLSyn miR-92 sponge (n= 7) rats 14 days after intraspinal inoculations. Error bars represent SEM. Unpaired t test, non-significant (ns).

3.1.2 Locomotor activity of STZ rats intraspinally inoculated with pLSyn and pLSyn miR-92 sponge lentiviral particles

As in Study 2, all animals were tested using the OFT to evaluate their locomotor activity. Again, there were no differences in their mobility after surgery, when comparing STZ pLSyn and STZ pLSyn miR-92 sponge rats (Figure 23).

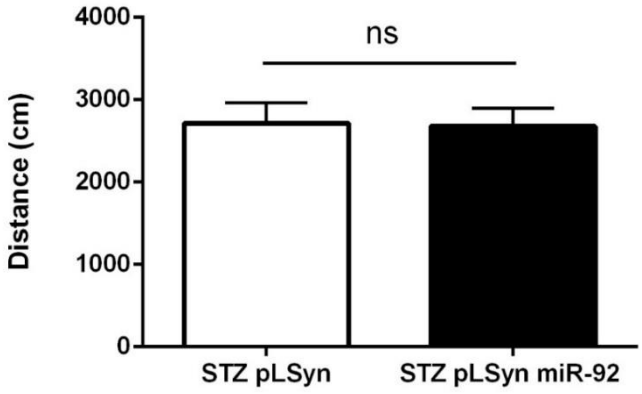

Figure 23 – Analysis of locomotor activity of inoculated STZ-diabetic rats after intraspinal surgery. OFT analysis 14 days after intraspinal injection of STZ pLSyn (n=6) and STZ pLSyn miR-92 sponge (n=7). Travelled distance in cm was calculated. Error bars represent SEM. Unpaired t test, non-significant (ns).

3.1.3 Effects of intrathecal administration of DIOA on the mechanical nociception of STZ rats inoculated with pLSyn or pLSyn-miR-92 sponge lentiviral particles

As shown in Figure 24, 30 min after the intrathecal injection of DIOA in STZ-diabetic rats inoculated with pLSyn-miR-92 sponge lentiviral particles, these animals presented decreased PWTs, i.e. increased mechanical nociception, when compared with the PWTs recorded at baseline (before DIOA administration). Further, these animals exhibited decreased PWTs 30 and 45 min after DIOA injection compared with their STZ pLSyn miR-92 counterparts that receive an intrathecal injection with vehicle solution only. Moreover, after DIOA injection, the PWTs of STZ pLSyn miR-92 rats did not differ from the PWTs exhibited by STZ rats inoculated with pLSyn alone and intrathecally injected with either DIOA or vehicle solution. Regarding the results of the intrathecal injection of DIOA in STZ-diabetic rats inoculated with pLSyn lentiviral particles, we observed that DIOA induced no effects on the PWTs of these animals (Figure 24).

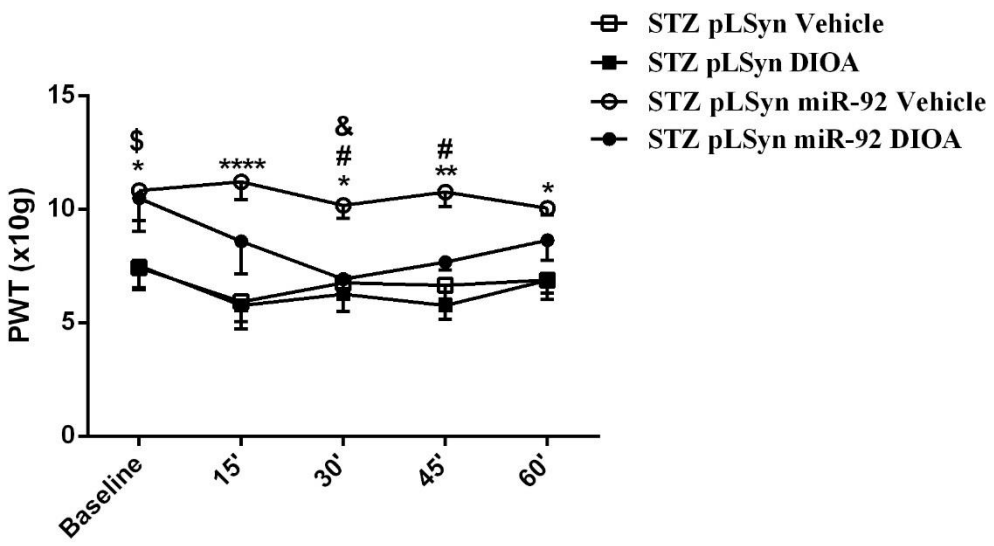

Figure 24 – Effect of KCC2 inhibitor, DIOA, on mechanical nociception of inoculated STZ-diabetic rats. STZ rats inoculated with pLSyn or pLSyn miR-92, injected with vehicle and DIOA were tested by the Randall-Selitto PPT. PWTs were recorded at 14 days after spinal lentiviral inoculation (Baseline), at 15', 30', 45' and 60' aft after intrathecal injection of vehicle or drug. Error bars represent SEM. Two-Way RM ANOVA, * corresponds to the comparison between both vehicle groups, *p<0,05, **p<0,01, ****p<0,001, # corresponds to the comparison between STZ pLSyn miR-92 Vehicle and STZ pLSyn miR-92 DIOA, #p<0,05, $ corresponds to the comparison between STZ pLSyn miR-92 DIOA with STZ pLSyn Vehicle and STZ pLSyn DIOA, $p<0,05, & corresponds to the comparison between STZ pLSyn miR-92 DIOA and respective baseline, &p<0,05.

3.1.4 Effects of intrathecal administration of BIC on the mechanical nociception of STZ rats inoculated with pLSyn or pLSyn-miR-92 sponge lentiviral particles

As can be seen in Figure 25, 30 min after the intrathecal injection of BIC in STZ-diabetic rats inoculated with pLSyn-miR-92 sponge lentiviral particles, these animals presented decreased PWTs, i.e. increased mechanical nociception, when compared with the PWTs recorded at baseline (before BIC administration). Further, these animals exhibited decreased PWTs 30 and 45 min after BIC injection compared with their STZ pLSyn miR-92 sponge counterparts that received an intrathecal injection of vehicle solution only. Furthermore, after BIC injection, the PWTs of STZ pLSyn miR-92 rats did not differ from the PWTs exhibited by STZ rats inoculated with pLSyn control lentiviral particles and intrathecally injected with vehicle solution. As to the results of the intrathecal injection of BIC in STZ-diabetic rats

inoculated with pLSyn control lentiviral particles, we observed that, 45 min post-BIC injection, these animals exhibited increased PWTs, i.e. decreased mechanical nociception, when compared with the PWTs recorded at baseline (before BIC administration). At this time point, STZ pLSyn rats injected intrathecally with BIC presented increased PWTs compared with STZ pLSyn rats that received an injection of vehicle solution only.

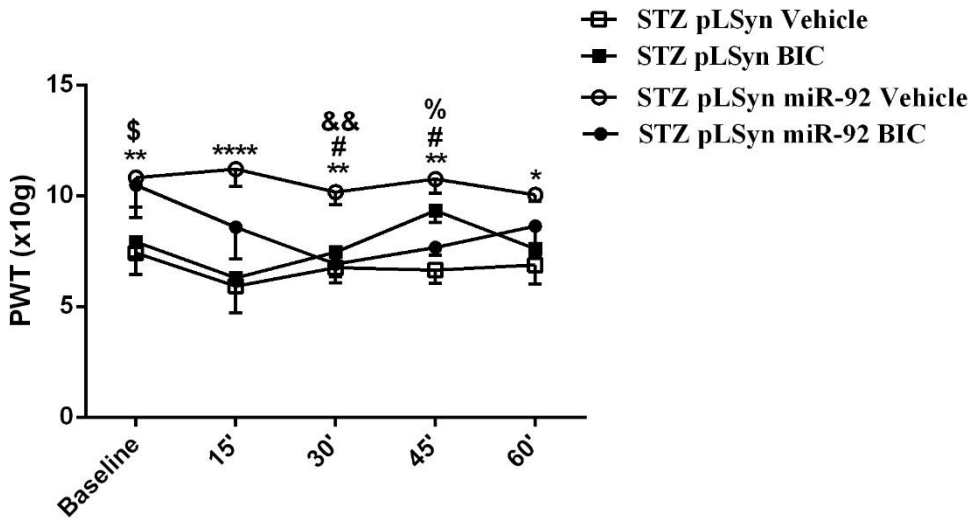

Figure 25 – Effect of $GABA_AR$ antagonist, BIC, on mechanical nociception of inoculated STZ-diabetic rats. STZ rats inoculated with pLSyn or pLSyn miR-92, injected with vehicle or BIC, were tested by the Randall-Selitto PPT. PWTs were recorded at 14 days after spinal lentiviral inoculation (Baseline), at 15', 30', 445' and 60' after intrathecal injection of vehicle or BIC. Error bars represent SEM. Two-Way RM ANOVA, * corresponds to the comparison between both vehicle groups, *p<0,05, **p<0,01, ****p<0,0001, # corresponds to the comparison between STZ pLSyn miR-92 Vehicle and STZ pLSyn miR-92 BIC, #<0,05, $ corresponds to the comparison between STZ pLSyn miR-92 BIC with STZ pLSyn Vehicle and STZ pLSyn BIC, $p<0,05, & corresponds to the comparison between STZ pLSyn miR-92 DIOA and respective baseline, &&p<0,01, % corresponds to the comparison between STZ pLSyn BIC with STZ pLSyn Vehicle and with respective baseline, % p<0,05.

4. Study 4: Effects of pro-inflammatory cytokines, TNF-α and IL-1β, on KCC2 expression in neuronal cultures (on-going experiments)

Microglia seems to be involved in PDN-induced KCC2 dysregulation, as the inhibition of its activity, achieved by an intrathecal administration of minocycline, a specific microglia inhibitor, restored spinal KCC2 expression and reversed mechanical hypersensitivity in STZ-diabetic rats (C. Morgado, P. Pereira-Terra, et al., 2011). The mechanisms by which microglia inhibition reverses these diabetic-induced changes are still elusive. Microglia-secreted brain-derived neurotrophic factor (BDNF) was shown to be involved in KCC2 deregulation in other chronic pain conditions (Coull et al., 2003), but not involved in PDN (C. Morgado, P. Pereira-Terra, et al., 2011; Wardle & Poo, 2003). Interestingly, minocycline was shown to decrease IL-1β and TNF-α levels in the spinal cord of STZ-diabetic rats, which were shown to be significantly upregulated (Cata, Weng, & Dougherty, 2008; Lee et al., 2003; C. Morgado, P. Pereira-Terra, et al., 2011). These findings raised the hypothesis that the reduction in IL-1β and TNF-α may be mediating the minocycline effects on spinal KCC2 expression in STZ-diabetic rats. However, the involvement of IL-1β and TNF-α in neuronal KCC2 expression was never addressed.

In order to understand if inflammation affects this cross talk between KCC2-miR-92, preliminary tests were made. Neuronal cultures from hippocampus and spinal cord were transfected with pro-inflammatory cytokines, and KCC2 protein levels were evaluated as well as miR-92 expression in hippocampal neurons (Figure 26). Since there are studies where GABA and KCC2 were related (Dai & Ma, 2014; Li, Li, Wei, Qu, & Wu, 2010; Morales-Aza, Chillingworth, Payne, & Donaldson, 2004; C. Morgado, P. Pereira-Terra, et al., 2011; Wardle & Poo, 2003; Z. Zhang, Wang, Wang, Lu, & Pan, 2013), the follow experiments were a pilot to understand which mechanism is underlying modulation of KCC2 and consequently GABA reversal.

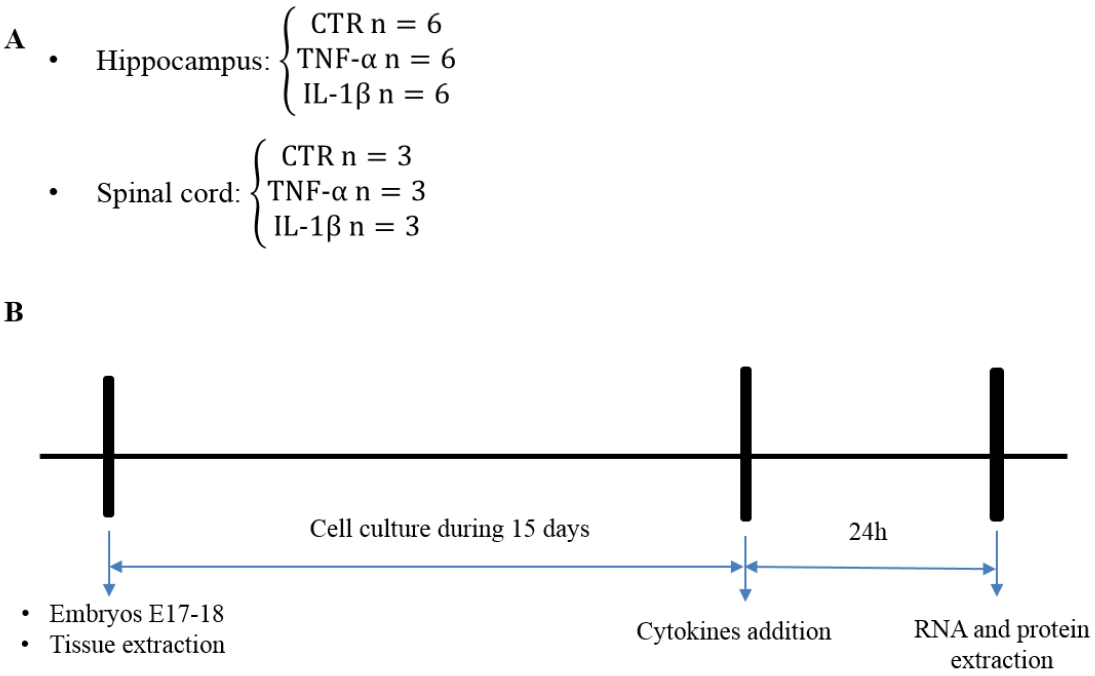

Figure 26 – Experimental design of Study 4: Effects of pro-inflammatory cytokines, TNF-α and IL-1β, on KCC2 expression in neuronal cultures (on-going experiments). (A) Experimental groups. **(B)** Timeline.

4.1 Study 4 Results

4.1.1 Effects of TNF-α and IL-1β in the of KCC2 mRNA and miR-92 in neuronal cultures

The expression of KCC2 mRNA and miR-92 was analyzed on hippocampal neuronal cultures after 24 hours of exposure to TNF-α and IL-1β. Both inflammatory mediators induced a significant decrease in the expression of KCC2 mRNA (Figure 27). No differences were detected in the expression of miR-92 (Figure 28).

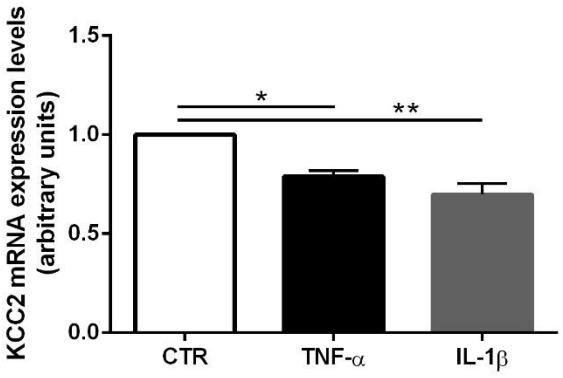

Figure 27 – Effects of TNF-α and IL-1β on KCC2 mRNA expression in hippocampal primary cultures. RT-PCR quantification of KCC2 mRNA expression levels, in hippocampal neurons cultured in normal medium (CTR) (n=3), in medium with the pro-inflammatory cytokine TNF-α (50ng/mL) (n=3), and in medium with the pro-inflammatory cytokine IL-1β (10 ng/mL) (n=3). Error bars represent SEM. One-Way ANOVA, n=3, * p<0,05, **p<0,01.

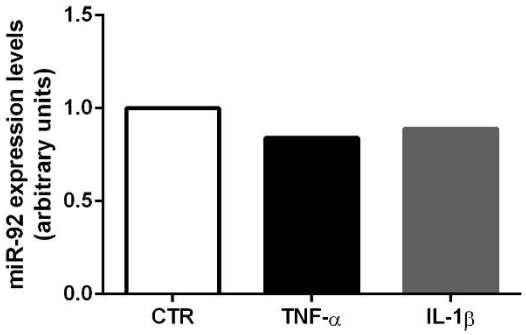

Figure 28 – Effects of TNF-α and IL-1β on miR-92 expression in hippocampal primary culture. RT-PCR quantification of miR-92 expression levels, in hippocampal neurons cultured in normal medium (CTR) (n=1), in medium with the pro-inflammatory cytokine TNF-α (50 ng/mL) (n=1), and in medium with the pro-inflammatory cytokine IL-1β (10 ng/mL) (n=1). No statistical analysis was made due to insufficient number of cultures.

4.1.2 KCC2 protein expression levels

The expression of KCC2 was evaluated in hippocampal and spinal cord neurons in the same pro-inflammatory conditions. In both neurons, the exposure to TNF-α and IL-1β tended to decrease KCC2 expression, although no statistical significant differences were reached

when compared with controls. The effects tended to be more pronounced in hippocampal than in spinal cord neurons (Figure 29 and 30, respectively).

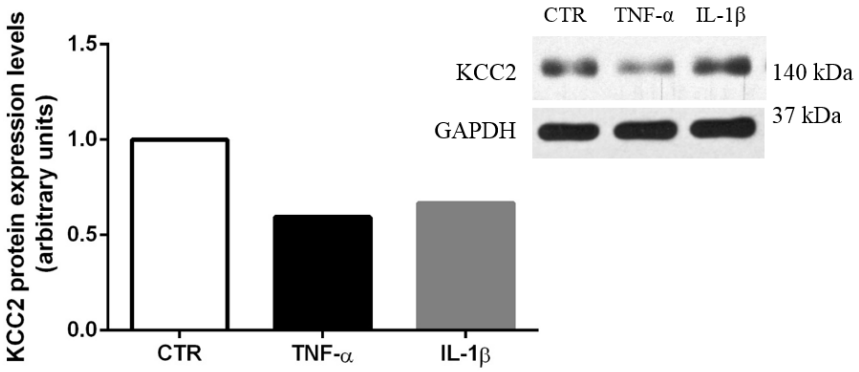

Figure 29 – Effects of TNF-α and IL-1β on KCC2 protein expression levels in hippocampal primary cultures. Expression levels of KCC2 protein in hippocampal neurons cultured in normal medium (CTR) (n=2), in medium with the pro-inflammatory cytokine TNF-α (50 ng/mL) (n=2), and in medium with the pro-inflammatory cytokine IL-1β (10 ng/mL) (n=2), by Western Blotting. No statistical analysis was made due to insufficient number of cultures.

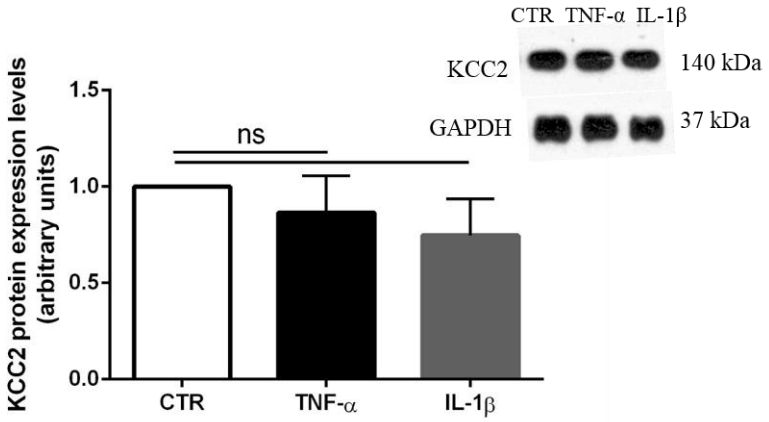

Figure 30 – Effects of TNF-α and IL-1β on KCC2 protein expression levels in spinal cord primary cultures. Expression levels of KCC2 protein in spinal cord neurons cultured in normal medium (CTR) (n=3), in medium with the pro-inflammatory cytokine TNF-α (50 ng/mL) (n=3), and in medium with the pro-inflammatory cytokine IL-1β (10 ng/mL) (n=3), by Western Blotting. Error bars represent SEM. One-Way ANOVA, non-significant (ns).

V. Discussion

In the present study we show, for the first time, that STZ-induced type 1 diabetic rats with PDN exhibit increased levels of miR-92 in the spinal cord L4-L5 segment compared with control animals. This result supports our hypothesis that the decreases in the levels of KCC2 protein observed in the spinal cord of different models of STZ-diabetic rats with PDN (Jolivalt et al., 2008; Lee-Kubli & Calcutt, 2014; C. Morgado, P. Pereira-Terra, et al., 2011; C. Morgado, P. Pereira-Terra, et al., 2011; Morgado et al., 2008) could be mediated by increases in the levels of miR-92. However, analysis of spinal cord KCC2 mRNA levels revealed no differences between STZ-diabetic and control rats. This came as an unexpected result since a study using a computational prediction-based studies approach showed that miR-92 has KCC2 mRNA as a target and, using cultures of cerebellar granule neurons, it showed that miR-92 directly modulates KCC2 protein expression (Barbato et al., 2010). Thus, our results suggest that, in PDN, miR-92 modulation of spinal cord KCC2 protein appears to involve mechanisms other than modulation of KCC2 mRNA. It is possible that miR-2 acts on other targets that may indirectly influence KCC2 protein levels. Such targets may be proteins involved in potential translational and post-translational mechanisms. So far, further to miR-92's association with KCC2, there are only a few studies describing other targets of miR-92, all related with tumorigenesis and the apoptotic pathway, such as the pro-apoptotic protein Bim (Al-Nakhle et al., 2010; Niu et al., 2012; Tsuchida et al., 2011; Ventura et al., 2008).

This study also shows that in STZ-diabetic rats with PDN, the selective inhibition of miR-92, by intraspinal injection of a miR-92 sponge lentiviral vectors (Barbato et al., 2010) increases the levels of KCC2 protein compared with STZ-diabetic animals that were not subjected to this miR-92 inhibition protocol. This result, besides confirming a role for spinal cord miR-92 in the regulation of KCC2 protein, further supports the effectiveness of the use of pLSyn miR-92 sponge lentiviral particles developed by Barbato and colleagues (Barbato et al., 2010; Vetere et al., 2014) in inhibiting actions previously demonstrated in the mouse hippocampus (Vetere et al., 2014). Moreover, we show that by inhibiting miR-92 in the spinal cord of STZ-diabetic rats, it was possible increase their

mechanical nociceptive thresholds when compared to STZ animals subjected to intraspinal injection of a control lentiviral vector only, suggesting that this procedure is able to decrease pain perception and could, therefore, be regarded as a potential future therapeutic strategy for pain relief in PDN and, perhaps, other painful disorders.

Considering that spinal cord KCC2 levels have a major role in the shift of GABA action, from inhibitory to excitatory, and that this change may be responsible for increased pain sensitivity in STZ-diabetic rats (Jolivalt et al., 2008; Morgado et al., 2008), a pharmacological study was undertaken in order to verify and further understand the crosstalk between KCC2 and GABA as possible mediators of the analgesic action of miR-92 inhibition. In normal conditions, KCC2 maintain cells' homeostasis extruding chloride and, consequently, modulating GABA effect to inhibitory (Fiumelli, Cancedda, & Poo, 2005; Rivera et al., 1999). In STZ-diabetic rats with PDN, it was shown that the opposite occurs, i.e. GABA effect is excitatory, due to decreases in spinal cord KCC2 levels (Morgado et al., 2008). In our study, the effects of miR-92 inhibition on pain responses to noxious mechanical stimulation were shown to be dependent on spinal KCC2 actions, as the intrathecal injection of DIOA, a specific KCC2 inhibitor, was shown to revert the analgesia induced by the inoculation of pLSyn-miR92 sponge lentiviral particles in the STZ-diabetic animals. Unexpectedly, injection of DIOA on STZ-diabetic rats inoculated with pLSyn had no effect on their PWTs, which may be due to possible limitations of the Randall-Selitto PPT and, therefore, it is critical to test this experiment with other mechanical nociception and tactile allodynia tests. Moreover, the inoculation of pLSyn-miR-92 sponge lentiviral particles in the STZ-diabetic animals was shown to restore the inhibitory post-synaptic role of GABA, as the intrathecal administration of BIC, a $GABA_AR$ antagonist, was shown to decrease the PWTs in these animals. On the contrary, BIC administration in STZ rats inoculated with pLSyn elicited an analgesic effect, showing that the post-synaptic role of GABA was excitatory and hyperalgesic in such condition. These findings corroborate the results from previous studies (Jolivalt et al., 2008), showing an analgesic effect of BIC in STZ rats and reinforce the role of KCC2 expression in the shift of GABA action from inhibition to excitation in spinal nociceptive neurotransmission in type 1 diabetic rats. The results of

this study allow us to conclude that decreased mechanical nociception exhibited by STZ-diabetic animals intraspinally inoculated with pLSyn miR-92 sponge lentiviral particles when compared to STZ animals inoculated with a control lentiviral vector is, indeed, mediated by increased KCC2 levels which, in turn, cause a shift in the action of GABA from excitatory to inhibitory.

The mechanisms leading to KCC2 deregulation during PDN are still not well understood. It is known that microglia activation contributes to KCC2 neuronal disruption in the spinal cord of diabetic rats with PDN (Daulhac et al., 2006; C. Morgado, P. Pereira-Terra, et al., 2011; Pabreja, Dua, Sharma, Padi, & Kulkarni, 2011; Talbot & Couture, 2012; Tsuda, Inoue, & Salter, 2005; Tsuda, Ueno, Kataoka, Tozaki-Saitoh, & Inoue, 2008; Wang, Couture, & Hong, 2014; Wodarski, Clark, Grist, Marchand, & Malcangio, 2009), although the mechanisms behind microglia contribution are still unknown. Our findings showed that KCC2 mRNA levels were significantly decreased in hippocampal neurons exposed to the pro-inflammatory cytokines, TNF-α and IL-1β, but only a tendency for a reduction was detected in KCC2 protein expression in the same experiments. It is important to stress that that KCC2 protein levels experiment is not conclusive given its preliminary nature (n=2). However, if confirmed, this result may be related to the time needed for KCC2 recycling at the plasma membrane. More precisely, while significant differences in KCC2 mRNA were already present 24h after IL-1β or TNF-α exposure, the effects on protein expression may occur latter or need a higher period of exposure to the pro-inflammatory mediators to occur. This lack of significant differences in KCC2 protein expression was also observed using the same experimental protocol in spinal cord neuronal cultures. It remains to evaluate if KCC2 mRNA expression is also affected by IL-1β and TNF-α in spinal cord neurons. In a single experiment we tested if miR-92 expression was altered by the exposure of hippocampal neurons to IL-1β and TNF-α. This very preliminary result indicated a slight reduction, which needs to be confirmed in future studies.

The completion of these *in vitro* studies may provide important clues on the possible role of inflammation on the disruption of spinal cord miR-92 and KCC2 levels in PDN.

In conclusion, this study strongly supports a role for miR-92 in the regulation of KCC2, providing new insights on the ethiopathology of PDN and opening new perspectives on novel

therapeutic approaches. Moreover, our results are of interest for the study and treatment of other neurological disorders associated with KCC2 disruption such as other chronic pain conditions and epilepsy (Dai & Ma, 2014; Palma et al., 2006; Rivera et al., 2002; Woo et al., 2002).

.

VI. References

Ahmad, S., & Mittal, M. Diabetic Neuropathies.

Al-Nakhle, H., Burns, P. A., Cummings, M., Hanby, A. M., Hughes, T. A., Satheesha, S., . . . Speirs, V. (2010). Estrogen receptor β1 expression is regulated by miR-92 in breast cancer. *Cancer research, 70*(11), 4778-4784.

Almeida, A., Leite-Almeida, H., & Tavares, I. (2006). Medullary control of nociceptive transmission: Reciprocal dual communication with the spinal cord. *Drug Discovery Today: Disease Mechanisms, 3*(3), 305-312. doi:http://dx.doi.org/10.1016/j.ddmec.2006.09.001

American Diabetes, A. (2009). Standards of medical care in diabetes—2009. *Diabetes Care, 32*(Supplement 1), S13-S61.

American Diabetes, A. (2014). Diagnosis and Classification of Diabetes Mellitus. *Diabetes Care, 37*(Supplement 1), S81-S90. doi:10.2337/dc14-S081

Andersen, H. H., Duroux, M., & Gazerani, P. (2014). MicroRNAs as modulators and biomarkers of inflammatory and neuropathic pain conditions. *Neurobiology of Disease, 71*, 159-168.

Balena, T., Acton, B. A., Koval, D., & Woodin, M. A. (2008). Extracellular potassium regulates the chloride reversal potential in cultured hippocampal neurons. *Brain research, 1205*, 12-20.

Barbato, C., Ruberti, F., Pieri, M., Vilardo, E., Costanzo, M., Ciotti, M. T., . . . Cogoni, C. (2010). MicroRNA-92 modulates K(+) Cl(−) co-transporter KCC2 expression in cerebellar granule neurons. *Journal of neurochemistry, 113*(3), 591-600. doi:10.1111/j.1471-4159.2009.06560.x

Bartel, D. P. (2004). MicroRNAs: Genomics, Biogenesis, Mechanism, and Function. *Cell, 116*(2), 281-297. doi:http://dx.doi.org/10.1016/S0092-8674(04)00045-5

Boulton, A. J. M., Vinik, A. I., Arezzo, J. C., Bril, V., Feldman, E. L., Freeman, R., . . . Ziegler, D. (2005). Diabetic neuropathies a statement by the American Diabetes Association. *Diabetes Care, 28*(4), 956-962.

Brandenburger, T., Castoldi, M., Brendel, M., Grievink, H., Schlösser, L., Werdehausen, R., . . . Hermanns, H. (2012). Expression of spinal cord microRNAs in a rat model of chronic neuropathic pain. *Neuroscience Letters, 506*(2), 281-286.

Calcutt, N. A. (2004). Modeling diabetic sensory neuropathy in rats *Pain Research* (pp. 55-65): Springer.

Callaghan, B. C., Cheng, H. T., Stables, C. L., Smith, A. L., & Feldman, E. L. (2012). Diabetic neuropathy: clinical manifestations and current treatments. *The Lancet Neurology, 11*(6), 521-534. doi:http://dx.doi.org/10.1016/S1474-4422(12)70065-0

Cata, J. P., Weng, H.-R., & Dougherty, P. M. (2008). The effects of thalidomide and minocycline on taxol-induced hyperalgesia in rats. *Brain research, 1229*, 100-110.

Chamma, I., Chevy, Q., Poncer, J. C., & Lévi, S. (2012). Role of the neuronal K-Cl co-transporter KCC2 in inhibitory and excitatory neurotransmission. *Frontiers in cellular neuroscience, 6*.

Cordero-Erausquin, M., Coull, J. A. M., Boudreau, D., Rolland, M., & De Koninck, Y. (2005). Differential maturation of GABA action and anion reversal potential in spinal lamina I neurons: impact of chloride extrusion capacity. *The Journal of Neuroscience, 25*(42), 9613-9623.

Coull, J. A. M., Boudreau, D., Bachand, K., Prescott, S. A., Nault, F., Sík, A., . . . De Koninck, Y. (2003). Trans-synaptic shift in anion gradient in spinal lamina I neurons as a mechanism of neuropathic pain. *Nature, 424*(6951), 938-942.

Courteix, C., Eschalier, A., & Lavarenne, J. (1993). Streptozocin-induced diabetic rats: behavioural evidence for a model of chronic pain. *PAIN, 53*(1), 81-88.

D'Mello, R., & Dickenson, A. H. (2008). Spinal cord mechanisms of pain. *British journal of anaesthesia, 101*(1), 8-16.

Dai, S., & Ma, Z. (2014). BDNF-trkB-KCC2-GABA pathway may be related to chronic stress-induced hyperalgesia at both the spinal and supraspinal level. *Medical Hypotheses, 83*(6), 772-774. doi:http://dx.doi.org/10.1016/j.mehy.2014.10.008

Daulhac, L., Mallet, C., Courteix, C., Etienne, M., Duroux, E., Privat, A.-M., . . . Fialip, J. (2006). Diabetes-induced mechanical hyperalgesia involves spinal mitogen-activated protein kinase activation in neurons and microglia via N-methyl-D-aspartate-dependent mechanisms. *Molecular Pharmacology, 70*(4), 1246-1254.

Diabetologia, S. P. d. (2014). *Diabetes: Factos e Números 2014*. www.spd.pt / diabetes@spd.pt / observatorio@spd.pt

Diseases, N. I. o. D., Digestive, & Kidney. (2015). Diabetic Neuropathies: The Nerve Damage of Diabetes. Retrieved from http://www.ncbi.nlm.nih.gov/pubmed/

Duby, J. J., Campbell, R. K., Setter, S. M., White, J. R., & Rasmussen, K. A. (2004). Diabetic neuropathy: an intensive review. *American Journal Of Health-System Pharmacy: AJHP: Official Journal Of The American Society Of Health-System Pharmacists, 61*(2), 160-173. Retrieved from http://search.ebscohost.com/login.aspx?direct=true&db=mdc&AN=14750401&lang=pt-br&site=ehost-live&scope=site

Dull, T., Zufferey, R., Kelly, M., Mandel, R. J., Nguyen, M., Trono, D., & Naldini, L. (1998). A third-generation lentivirus vector with a conditional packaging system. *Journal of virology, 72*(11), 8463-8471.

Dyck, P. J., Albers, J. W., Andersen, H., Arezzo, J. C., Biessels, G. J., Bril, V., . . . Russell, J. W. (2011). Diabetic polyneuropathies: update on research definition, diagnostic criteria and estimation of severity. *Diabetes/Metabolism Research and Reviews, 27*(7), 620-628.

Fernandez-Valverde, S. L., Taft, R. J., & Mattick, J. S. (2011). MicroRNAs in β-cell biology, insulin resistance, diabetes and its complications. *Diabetes, 60*(7), 1825-1831.

Fiumelli, H., Cancedda, L., & Poo, M.-m. (2005). Modulation of GABAergic Transmission by Activity via Postsynaptic Ca2+-Dependent Regulation of KCC2 Function. *Neuron, 48*(5), 773-786. doi:http://dx.doi.org/10.1016/j.neuron.2005.10.025

Gardete-Correia, L., Boavida, J. M., Raposo, J. F., Mesquita, A. C., Fona, C., Carvalho, R., & Massano-Cardoso, S. (2010). First diabetes prevalence study in Portugal: PREVADIAB study. *Diabetic Medicine, 27*(8), 879-881.

Guariguata, L., Whiting, D., Hambleton, I., Beagley, J., Linnenkamp, U., & Shaw, J. (2014). Global estimates of diabetes prevalence for 2013 and projections for 2035. *Diabetes research and clinical practice, 103*(2), 137-149.

Guay, C., Roggli, E., Nesca, V., Jacovetti, C., & Regazzi, R. (2011). Diabetes mellitus, a microRNA-related disease? *Translational Research, 157*(4), 253-264. doi:http://dx.doi.org/10.1016/j.trsl.2011.01.009

He, L., & Hannon, G. J. (2004). MicroRNAs: small RNAs with a big role in gene regulation. *Nature Reviews Genetics, 5*(7), 522-531.

Jolivalt, C. G., Lee, C. A., Ramos, K. M., & Calcutt, N. A. (2008). Allodynia and hyperalgesia in diabetic rats are mediated by GABA and depletion of spinal potassium-chloride co-transporters. *PAIN, 140*(1), 48-57. doi:http://dx.doi.org/10.1016/j.pain.2008.07.005

Kato, M., Castro, N. E., & Natarajan, R. (2013). MicroRNAs: potential mediators and biomarkers of diabetic complications. *Free Radical Biology and Medicine, 64*, 85-94.

Kazamel, M., & Dyck, P. J. (2015). Sensory manifestations of diabetic neuropathies: Anatomical and clinical correlations. *Prosthetics and orthotics international, 39*(1), 7-16.

Kress, M., Hüttenhofer, A., Landry, M., Kuner, R., Favereaux, A., Greenberg, D., . . . Malcangio, M. (2013). microRNAs in nociceptive circuits as predictors of future clinical applications. *Frontiers in molecular neuroscience, 6*.

Kusuda, R., Cadetti, F., Ravanelli, M. I., Sousa, T. A., Zanon, S., De Lucca, F. L., & Lucas, G. (2011). Differential expression of microRNAs in mouse pain models. *Mol Pain, 7*(17), 1744-8069.

Lamster, I. B. (2014). *Diabetes mellitus and oral health: an interprofessional approach*: John Wiley & Sons.

Lavertu, G., Côté, S. L., & De Koninck, Y. (2013). Enhancing K–Cl co-transport restores normal spinothalamic sensory coding in a neuropathic pain model. *Brain*. doi:10.1093/brain/awt334

Lawrie, C. H. (2013). *MicroRNAs in medicine*: John Wiley & Sons.

Lee-Kubli, C. A. G., & Calcutt, N. A. (2014). Altered rate-dependent depression of the spinal H-reflex as an indicator of spinal disinhibition in models of neuropathic pain. *PAIN®, 155*(2), 250-260. doi:http://dx.doi.org/10.1016/j.pain.2013.10.001

Lee, S. M., Yune, T. Y., Kim, S. J., Park, D. W., Lee, Y. K., Kim, Y. C., . . . Oh, T. H. (2003). Minocycline reduces cell death and improves functional recovery after traumatic spinal cord injury in the rat. *Journal of neurotrauma, 20*(10), 1017-1027.

Lenzen, S. (2008). The mechanisms of alloxan-and streptozotocin-induced diabetes. *Diabetologia, 51*(2), 216-226.

Li, Y.-Q., Li, H., Wei, J., Qu, L., & Wu, L.-a. (2010). Expression changes of K+–Cl− co-transporter 2 and Na+–K+–Cl− co-transporter1 in mouse trigeminal subnucleus caudalis following pulpal inflammation. *Brain research bulletin, 81*(6), 561-564.

Mantyh, P. W., & Hunt, S. P. (2004). Setting the tone: superficial dorsal horn projection neurons regulate pain sensitivity. *Trends in Neurosciences, 27*(10), 582-584.

McMahon, S., Koltzenburg, M., Tracey, I., & Turk, D. C. (2013). *Wall & Melzack's textbook of pain*: Elsevier Health Sciences.

Morales-Aza, B. M., Chillingworth, N. L., Payne, J. A., & Donaldson, L. F. (2004). Inflammation alters cation chloride cotransporter expression in sensory neurons. *Neurobiology of Disease, 17*(1), 62-69. doi:http://dx.doi.org/10.1016/j.nbd.2004.05.010

Morgado, C., Pereira-Terra, P., Cruz, C. D., & Tavares, I. (2011). Minocycline completely reverses mechanical hyperalgesia in diabetic rats through microglia-induced changes in the expression of the potassium chloride co-transporter 2 (KCC2) at the spinal cord. *Diabetes, Obesity & Metabolism, 13*(2), 150-159. doi:10.1111/j.1463-1326.2010.01333.x

Morgado, C., Pereira-Terra, P., & Tavares, I. (2011). α-Lipoic acid normalizes nociceptive neuronal activity at the spinal cord of diabetic rats. *Diabetes, Obesity and Metabolism, 13*(8), 736-741.

Morgado, C., Pinto-Ribeiro, F., & Tavares, I. (2008). Diabetes affects the expression of GABA and potassium chloride cotransporter in the spinal cord: A study in streptozotocin diabetic rats. *Neuroscience Letters, 438*(1), 102-106. doi:http://dx.doi.org/10.1016/j.neulet.2008.04.032

Morgado, C., Silva, L., Pereira-Terra, P., & Tavares, I. (2011). Changes in serotoninergic and noradrenergic descending pain pathways during painful diabetic neuropathy: the preventive action of IGF1. *Neurobiology of Disease, 43*(1), 275-284.

Niu, H., Wang, K., Zhang, A., Yang, S., Song, Z., Wang, W., . . . Wang, Y. (2012). miR-92a is a critical regulator of the apoptosis pathway in glioblastoma with inverse expression of BCL2L11. *Oncology reports, 28*(5), 1771-1777.

Ossipov, M. H., Dussor, G. O., & Porreca, F. (2010). Central modulation of pain. *The Journal of Clinical Investigation, 120*(11), 3779-3787. doi:10.1172/JCI43766

Pabreja, K., Dua, K., Sharma, S., Padi, S. S., & Kulkarni, S. K. (2011). Minocycline attenuates the development of diabetic neuropathic pain: possible anti-inflammatory and anti-oxidant mechanisms. *European Journal of Pharmacology, 661*(1), 15-21.

Palma, E., Amici, M., Sobrero, F., Spinelli, G., Di Angelantonio, S., Ragozzino, D., . . . Miledi, R. (2006). Anomalous levels of Cl− transporters in the hippocampal subiculum from temporal lobe epilepsy patients make GABA excitatory. *Proceedings of the National Academy of Sciences, 103*(22), 8465-8468.

Peltier, A., Goutman, S. A., & Callaghan, B. C. (2014). Painful diabetic neuropathy. *BmJ, 348*.

Pogatzki, E. M., Urban, M. O., Brennan, T. J., & Gebhart, G. F. (2002). Role of the rostral medial medulla in the development of primary and secondary hyperalgesia after incision in the rat. *Anesthesiology, 96*(5), 1153-1160.

Porreca, F., Ossipov, M. H., & Gebhart, G. F. (2002). Chronic pain and medullary descending facilitation. *Trends in Neurosciences, 25*(6), 319-325. doi:http://dx.doi.org/10.1016/S0166-2236(02)02157-4

Price, T. J., Cervero, F., & de Koninck, Y. (2005). Role of cation-chloride-cotransporters (CCC) in pain and hyperalgesia. *Current topics in medicinal chemistry, 5*(6), 547.

Randall, L. O., & Selitto, J. J. (1957). A method for measurement of analgesic activity on inflamed tissue. *Arch Int Pharmacodyn Ther, 111*(4), 409-419. Retrieved from http://www.ncbi.nlm.nih.gov/pubmed/13471093

Rivera, C., Li, H., Thomas-Crusells, J., Lahtinen, H., Viitanen, T., Nanobashvili, A., . . . Kaila, K. (2002). BDNF-induced TrkB activation down-regulates the K+–Cl− cotransporter KCC2 and impairs neuronal Cl− extrusion. *The Journal of cell biology, 159*(5), 747-752.

Rivera, C., Voipio, J., Payne, J. A., Ruusuvuori, E., Lahtinen, H., Lamsa, K., . . . Kaila, K. (1999). The K+/Cl- co-transporter KCC2 renders GABA hyperpolarizing during neuronal maturation. *Nature, 397*(6716), 251-255. doi:http://www.nature.com/nature/journal/v397/n6716/suppinfo/397251a0_S1.html

Ruberti, F., Barbato, C., & Cogoni, C. (2012). Targeting microRNAs in neurons: tools and perspectives. *Experimental Neurology, 235*(2), 419-426.

Sakai, A., & Suzuki, H. (2014). Emerging roles of microRNAs in chronic pain. *Neurochemistry international, 77*, 58-67.

Shakeel, M. (2014). Recent advances in understanding the role of oxidative stress in diabetic neuropathy. *Diabetes & Metabolic Syndrome: Clinical Research & Reviews*.

Shantikumar, S., Caporali, A., & Emanueli, C. (2012). Role of microRNAs in diabetes and its cardiovascular complications. *Cardiovascular research, 93*(4), 583-593.

Skyler, J. S. (2004). Diabetes mellitus: pathogenesis and treatment strategies. *Journal of medicinal chemistry, 47*(17), 4113-4117.

Stahl, S. M. (2013). Stahl's essential psychopharmacology: neuroscientific basis and practical applications: Cambridge university press.

Stil, A., Liabeuf, S., Jean-Xavier, C., Brocard, C., Viemari, J. C., & Vinay, L. (2009). Developmental up-regulation of the potassium–chloride cotransporter type 2 in the rat lumbar spinal cord. *Neuroscience, 164*(2), 809-821.

Szkudelski, T. (2001). The mechanism of alloxan and streptozotocin action in B cells of the rat pancreas. *Physiological research, 50*(6), 537-546.

Talbot, S., & Couture, R. (2012). Emerging role of microglial kinin B1 receptor in diabetic pain neuropathy. *Experimental Neurology, 234*(2), 373-381.

Tavares, I., Lima, D., & Almeida, A. (2014). Neurobiologia da Dor: Mecanismos de Transmissão e Modulação da Informação Nociceptiva. *Dor, 22*(4).

Taylor, B. K. (2009). Spinal inhibitory neurotransmission in neuropathic pain. *Current pain and headache reports, 13*(3), 208-214.

Tesfaye, S., Boulton, A. J. M., & Dickenson, A. H. (2013). Mechanisms and Management of Diabetic Painful Distal Symmetrical Polyneuropathy. *Diabetes Care, 36*(9), 2456-2465. doi:10.2337/dc12-1964

Tesfaye, S., Boulton, A. J. M., Dyck, P. J., Freeman, R., Horowitz, M., Kempler, P., . . . on behalf of the Toronto Diabetic Neuropathy Expert, G. (2010). Diabetic Neuropathies: Update on Definitions, Diagnostic Criteria, Estimation of Severity, and Treatments. *Diabetes Care, 33*(10), 2285-2293. Retrieved from http://care.diabetesjournals.org/content/33/10/2285.abstract

Tesfaye, S., & Selvarajah, D. (2012). Advances in the epidemiology, pathogenesis and management of diabetic peripheral neuropathy. *Diabetes/Metabolism Research and Reviews, 28*(S1), 8-14.

Tesfaye, S., Vileikyte, L., Rayman, G., Sindrup, S. H., Perkins, B. A., Baconja, M., . . . Boulton, A. J. M. (2011). Painful diabetic peripheral neuropathy: consensus recommendations on diagnosis, assessment and management. *Diabetes/Metabolism Research and Reviews, 27*(7), 629-638.

Tesfaye, S., Vileikyte, L., Rayman, G., Sindrup, S. H., Perkins, B. A., Baconja, M., . . . on behalf of The Toronto Expert Panel on Diabetic, N. (2011). Painful diabetic peripheral neuropathy: consensus recommendations on diagnosis, assessment and management. *Diabetes/Metabolism Research and Reviews, 27*(7), 629-638. doi:10.1002/dmrr.1225

Tsuchida, A., Ohno, S., Wu, W., Borjigin, N., Fujita, K., Aoki, T., . . . Kuroda, M. (2011). miR-92 is a key oncogenic component of the miR-17–92 cluster in colon cancer. *Cancer science, 102*(12), 2264-2271.

Tsuda, M., Inoue, K., & Salter, M. W. (2005). Neuropathic pain and spinal microglia: a big problem from molecules in 'small' glia. *Trends in Neurosciences, 28*(2), 101-107. doi:http://dx.doi.org/10.1016/j.tins.2004.12.002

Tsuda, M., Ueno, H., Kataoka, A., Tozaki-Saitoh, H., & Inoue, K. (2008). Activation of dorsal horn microglia contributes to diabetes-induced tactile allodynia via extracellular signal-regulated protein kinase signaling. *Glia, 56*(4), 378-386.

Ventura, A., Young, A. G., Winslow, M. M., Lintault, L., Meissner, A., Erkeland, S. J., . . . Stone, J. R. (2008). Targeted deletion reveals essential and overlapping functions of the miR-17∼ 92 family of miRNA clusters. *Cell, 132*(5), 875-886.

Vetere, G., Barbato, C., Pezzola, S., Frisone, P., Aceti, M., Ciotti, M., . . . Ruberti, F. (2014). Selective inhibition of miR-92 in hippocampal neurons alters contextual fear memory. *Hippocampus, 24*(12), 1458-1465.

Vilardo, E., Barbato, C., Ciotti, M., Cogoni, C., & Ruberti, F. (2010). MicroRNA-101 regulates amyloid precursor protein expression in hippocampal neurons. *Journal of Biological Chemistry, 285*(24), 18344-18351.

Wang, D., Couture, R., & Hong, Y. (2014). Activated microglia in the spinal cord underlies diabetic neuropathic pain. *European Journal of Pharmacology, 728*(0), 59-66. doi:http://dx.doi.org/10.1016/j.ejphar.2014.01.057

Wardle, R. A., & Poo, M.-m. (2003). Brain-derived neurotrophic factor modulation of GABAergic synapses by postsynaptic regulation of chloride transport. *The Journal of Neuroscience, 23*(25), 8722-8732.

Wodarski, R., Clark, A. K., Grist, J., Marchand, F., & Malcangio, M. (2009). Gabapentin reverses microglial activation in the spinal cord of streptozotocin-induced diabetic rats. *European Journal of Pain, 13*(8), 807-811.

Woo, N. S., Lu, J., England, R., McClellan, R., Dufour, S., Mount, D. B., . . . Delpire, E. (2002). Hyperexcitability and epilepsy associated with disruption of the mouse neuronal-specific K–Cl cotransporter gene. *Hippocampus, 12*(2), 258-268.

Zeilhofer, H. U. (2008). Loss of glycinergic and GABAergic inhibition in chronic pain—contributions of inflammation and microglia. *International Immunopharmacology, 8*(2), 182-187. doi:http://dx.doi.org/10.1016/j.intimp.2007.07.009

Zhang, W., Liu, L. Y., & Xu, T. L. (2008). Reduced potassium-chloride co-transporter expression in spinal cord dorsal horn neurons contributes to inflammatory pain hypersensitivity in rats. *Neuroscience, 152*(2), 502-510. doi:http://dx.doi.org/10.1016/j.neuroscience.2007.12.037

Zhang, Z., Wang, X., Wang, W., Lu, Y.-G., & Pan, Z. Z. (2013). Brain-Derived Neurotrophic Factor–Mediated Downregulation of Brainstem K+–Cl– Cotransporter and Cell-Type–Specific GABA Impairment for Activation of Descending Pain Facilitation. *Molecular Pharmacology*, *84*(4), 511-520. Retrieved from http://molpharm.aspetjournals.org/content/84/4/511.abstractN2

Zhao, J., Lee, M.-C., Momin, A., Cendan, C.-M., Shepherd, S. T., Baker, M. D., . . . Perkins, J. R. (2010). Small RNAs control sodium channel expression, nociceptor excitability, and pain thresholds. *The Journal of Neuroscience*, *30*(32), 10860-10871.

Zimmermann, M. (1983). Ethical guidelines for investigations of experimental pain in conscious animals. *PAIN*, *16*(2), 109-110.

ATTACHMENTS

Recipes

1. Phosphate buffered saline (PBS) (1 L):

   PB 0.4 M pH=7.2 – 250 mL

   NaCl – 9 g

   H_2O up to 1L

2. Tris-Glycine-SDS (TGS 1X) (500mL):

   Tris-glycine – 50 mL

   SDS 0,1% – 5 mL

   H_2O up to 500 mL

3. Tris-Glycine (TG) 1X with 20% Methanol (500mL):

   Tris-glycine – 50 mL

   Methanol – 100 mL

4. Phosphate buffered saline with Triton X-100 (PBS-T) (1 L):

   PBS – 900 mL

   Triton X – 100 mL

5. Phosphate buffered saline with Tween 20 (PBS/T) (1 L):

   PBS-T 25X – 20 mL
   Tween 20 – 500 µL

   H_2O up to 1L

6. Transfer buffer (10X) (1 L):

   Glycine – 29.3 g

   Tris base – 58.15 g

   10% SDS – 37.5 mL

   H_2O up to 1L

7. Transfer Buffer with 20% Methanol (1 L):

   Transfer buffer 10X – 100 mL

Methanol – 200 mL

H_2O up to 1L

8. Tissues – 4x SDS-PAGE sample buffer:

   240 mM Tris/HCl pH 6.8

   40% glycerol

   8% SDS

   0.04% bromophenol blue – tiny bit

   10% β-Mercaptoethanol – added just before protein sample use

9. Tissues – Lysis buffer:

   20 M MOPS, pH 7.0;

   2 mM EGTA;

   5 mM EDTA;

   1% Triton X-100

   1% Phosphatase inhibitor cocktail 2 (Sigma-Aldrich, St. Louis, MO)

   1% Phosphatase inhibitor cocktail 3 (Sigma-Aldrich, St. Louis, MO)

   1% Proteases inhibitor (Sigma-Aldrich, St. Louis, MO)

10. Cell culture – 2X Laemmli loading buffer:

    125 mM tris-HCL pH6.8

    4% SDS

    20% glycerol

    0,04% bromophenol blue – tiny bit

    10% β-Mercaptoethanol – added just before protein sample use

11. Cell culture – Lysis buffer:

    1% Triton

    0,25% SDS

    1% Sodium Deoxycholate

    2mM EDTA

    1mM DTT

    Fresh phosphatase and protease inhibitors

12. Ponceau solution (1X):

Ponceau – 0.2 %

Trichloroacetic acid – 3 %

Sulphosalicylic acid – 3%

Western-Blotting Protocol for Tissues:

1. Preparation of samples homogenates:

   - Dissect the tissue of interest and quickly transfer to dry ice to prevent tissue degradation;
   - Store samples at -80°C for posterior use or keep on ice for immediate homogenization;
   - For a ~200 mg of tissue, add ~1000 µl lysis buffer rapidly to the tube, homogenize with ~75% of lysis buffer with a mechanical homogenizer, rinse one time with the remainder lysis buffer;
   - Incubate on ice about 20 min;
   - Centrifuge for 20 min at 21100xg at 4 ºC;
   - Transfer the supernatant to a fresh tube kept on ice and discard the pellet;
   - Centrifuge again for 10 min at 21100xg at 4 ºC and collect the supernatant to another tube;
   - Store the homogenates at -80 ºC.

2. Sample preparation:

   - Remove a small volume of lysate to perform a protein assay using the standard protocol of Bradford to determine the protein concentration; Bovine serum albumin (BSA) should be used as the protein standard;
   - Add to final protein concentration, 1X Sodium Dodecyl Sulphate (SDS) sample buffer, distilled H_2O and β-Mercaptoethanol
   - Boil each tissue homogenate with sample buffer at 100 ºC for 5 min;
   - Store homogenates at -20 ºC until use;
   - In the moment of use, homogenates should be rapidly defrosted at 37°C and centrifuge at max speed in a microcentrifuge;

3. Determination of the Protein Concentration:

   -Prepare protein standard in buffer ranging from 0 –1.5 mg/ml using a BSA standard;
   - In 96 well plate, add 5 µl of homogenate, previously thawed;
   - Add 250 µl of Bradford reagent in each well and mix gently for 30 seconds;
   - Let the samples incubate at room temperature for 5–45 min;
   - Measure the absorbance at 595 nm;
   - Plot the net absorbance vs. the protein concentration of each standard;

- Determine the protein concentration of the unknown samples by comparing the A595 values against the standard curve.

4. SDS-PAGE and electrophoresis
   - Prepare the resolving gel (8%) (1 gel)
     Acrylamide (40%) – 1,5 mL
     Gel buffer – 1,875 mL
     H2O d – 4,125 mL
     SDS 10% – 75 µL
     TEMED – 3,75 µl
     APS (10%) – 75 µl
   - Prepare the stacking gel (6%) (1 gel):
     Acrylamide (40%) – 563 µL
     Gel buffer – 938 µL
     H_2O – 2,063 mL
     SDS 10% – 37,5 µL
     TEMED – 3 µl
     APS (10%) – 75 µl
   - Load equal amounts of protein into each well of the SDS-PAGE gel. Load of 40 µg of total protein from each samples;
   - Electrophoresis is performed during 1 to 2 hours at 20 mA;

5. Protein transfer to nitrocellulose membranes:
   - Immerse sponges, filter papers and nitrocellulose membranes in 1X transfer buffer with 20% methanol;
   - Prepare the transfer stack as follows:
   (+) sponge - filter paper - nitrocellulose membrane - gel - filter paper - sponge (-)
   - Transfer the protein, by electroblotting, at 30 V overnight with stacks totally immersed in transfer buffer with 20% methanol;
   - Check protein transfer quality by staining the membranes with Ponceau solution.

6. Immunodetection of specific proteins:
   - Incubate the membranes with primary antibody for 1 overnight at 4 ºC;
   - Rinse with PBS/T;
   - Incubate with secondary antibody with blocking buffer (5% skimmed milk with PBS/T) for 1 hour;

- Rinse with PBS/T for 30 min (3x10 min);

- Incubate with Clarity™ Western ECL Substrate (BioRad, Portugal) (two compounds in the ratio 1:1) for 5 min;

- The signal is detected by ChemiDoc XRS + system (BioRad, Portugal).

Cultured cells

1. Protein Extraction:

   - Add 70 uL of Lysis buffer to each dish (35mm);

   - On ice, wash each dish with PBS 1X twice;

   - Add lysis buffer and scrape. (Save some lysis buffer for quantitation);

   - Collect to in a new tube and incubate for 30 min on ice;

   - Store at -80ºC.

   - To have a complete cell lysis, make some "freeze and thaw" cycles: thaw on ice, centrifuge at 12000xg for 20 min at 4ºC, collect to in a new tube, put at -80ºC for 20-30 min. Repeat until the lysate is clear and liquid (not gluey).

2. Determination of Protein Concentration:

   - Prepare protein standard in buffer ranging from 0 –1 mg/ml using a BSA standard (10mg/mL);

   - Prepare solution A': 20 uL reagent S/ 1mL reagent A.

   - DC Assay – Standards: 100 uL standard + 100 uL solution A' + 800 uL solution B

   - DC Assay – Samples: 98 uL H20 + 2 uL Sample + 100 uL solution A' + 800 uL solution B. Samples in duplicate

   - Read samples absorbance on Biospectophotometer.

RT-PCR Protocol:

1. RNA extraction:

   - Always on ice, remove growth media;

   - Wash with PBS;

   - On the hood, add 1mL of TRIzol in the cells. Lyse the cells directly in the culture dish by pipetting up and down several times;

   - Continue RNA isolation procedure according to TRIzol Reagent manufacturing instructions.

2. DNAse Treatment:

   - DNAse treatment and removal reagents according to TURBO DNA-free Kit manufacturing instructions.

3. Reverse Transcription and RT-PCR:

   - For mRNA, perform reverse transcription according to SYBR Green Kit manufacturer's instructions.

   - For microRNA, perform reverse transcription according to TaqMan Kit manufacturer's instructions.